Enhanced Pool Boiling of Water with Open Microchannels over Cylindrical Tubes

Master of Science – Thesis Presentation

Jeet S. Mehta

Thermal Analysis, Microfluidics, and Fuel Cell Laboratory

Department of Mechanical Engineering

Thesis Advisor: Satish G. Kandlikar

February 1, 2013

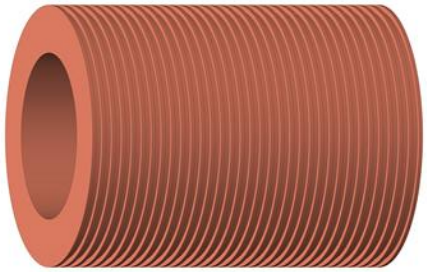

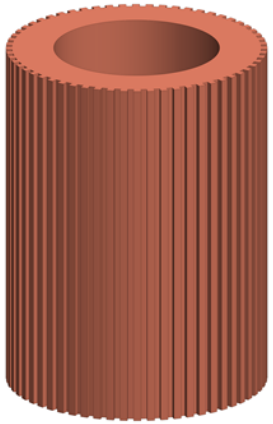

Outline

- Introduction
- Literature Review
- Objectives
- Approach
- Results and Discussions
- Conclusions
- Future Work

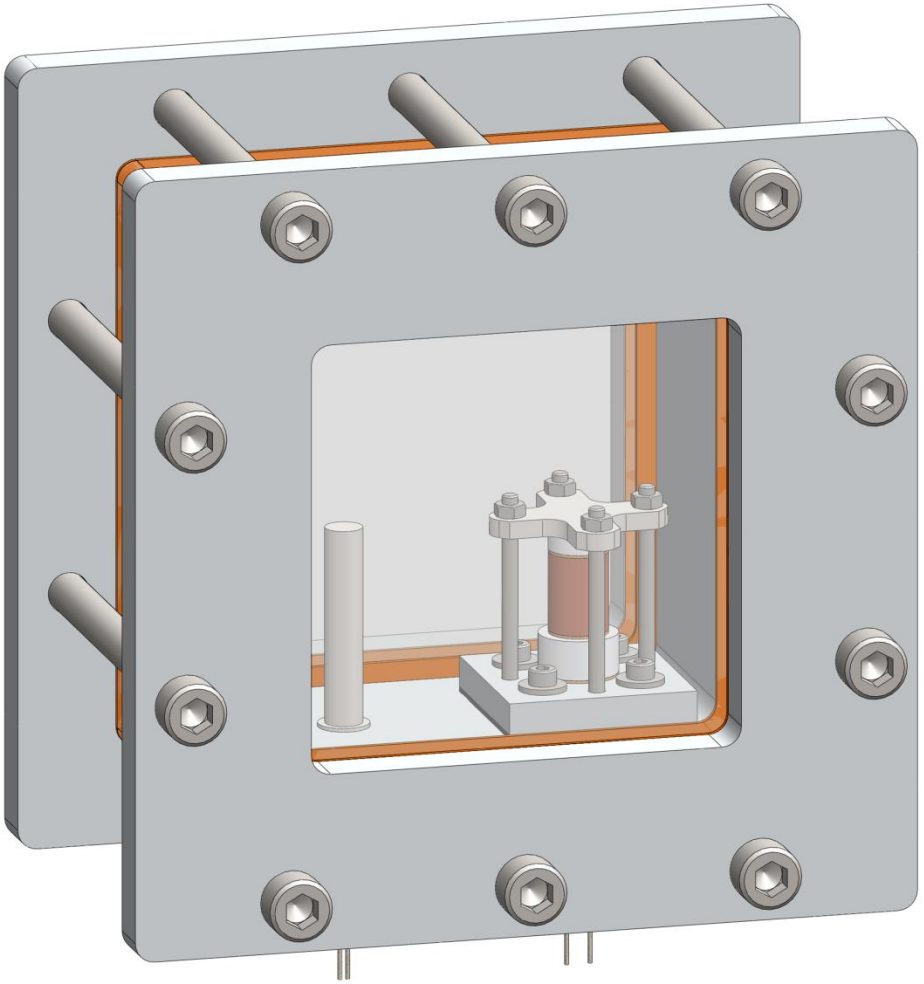

3D CAD model of experimental setup
with test surface in the vertical orientation

Introduction

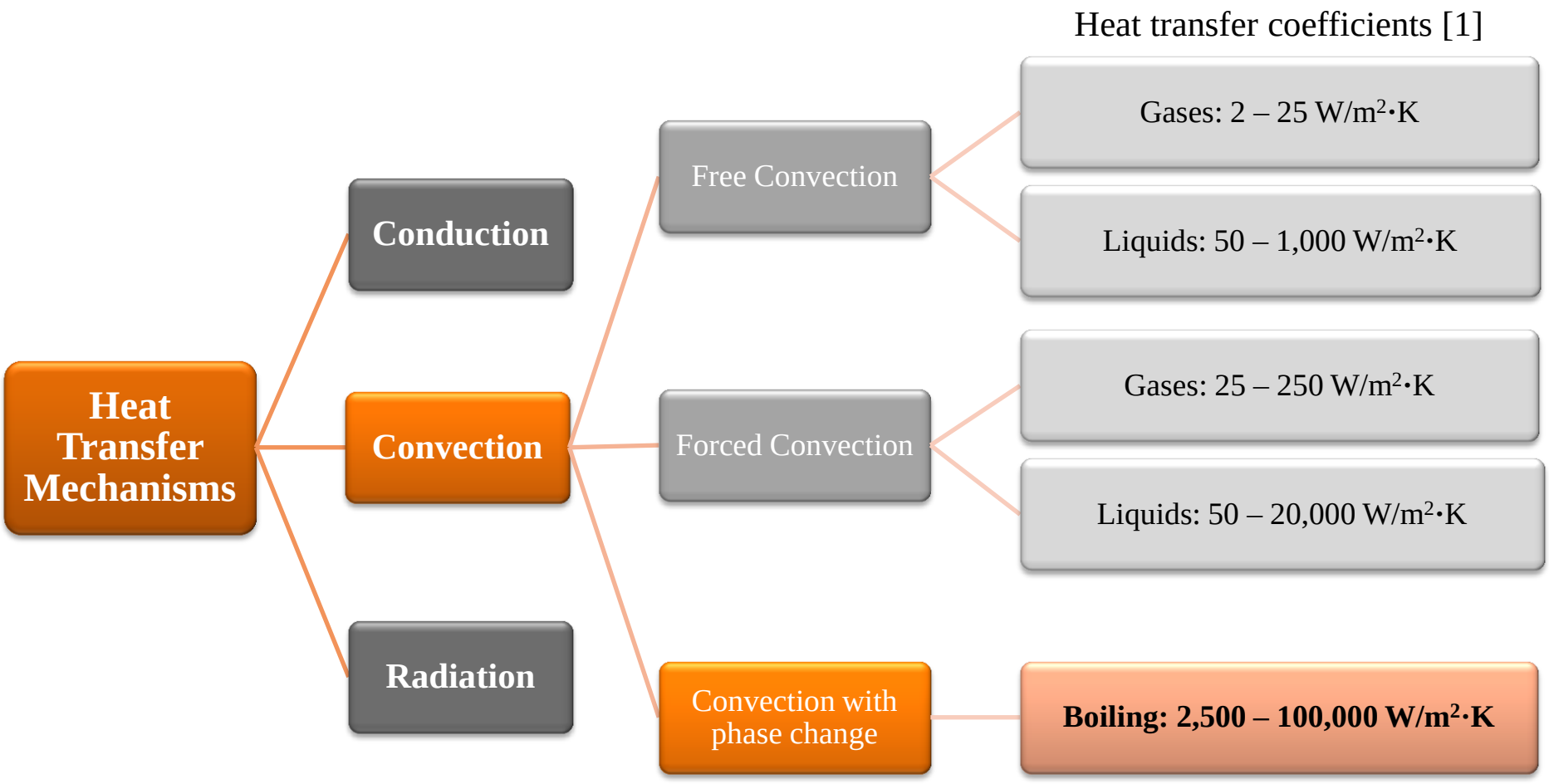

Heat Transfer through Boiling

- Ability to remove large quantities of heat
- Relatively small surface
- Latent heat of vaporization of the fluid
  - Responsible for the high heat transfer coefficients
- Boiling mechanisms
  - Flow boiling
    - Motion and mixing of liquid induced by external forces
    - Active technique: External power
  - Pool boing
    - Motion and mixing of liquid induced by free convection and bubble movement
    - Passive technique: No moving parts and cost effective

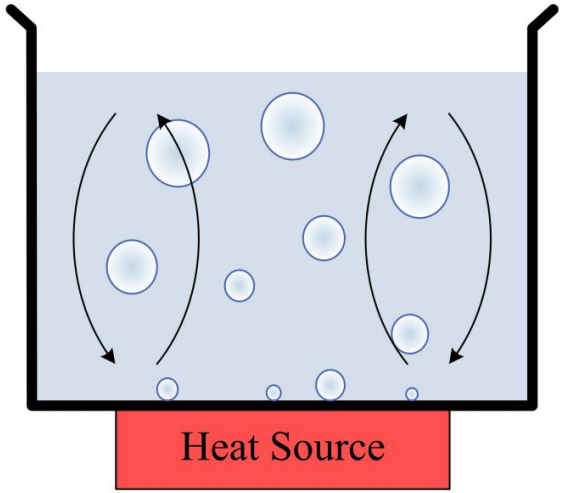

Pool Boiling

- Boiling applications
  - Fire-tube boilers / steam generators
  - Fusion reactors
  - Two phase heat exchangers and evaporators
  - Compact micro-scale heat exchangers

Typical Boiling Curve for Water [2]

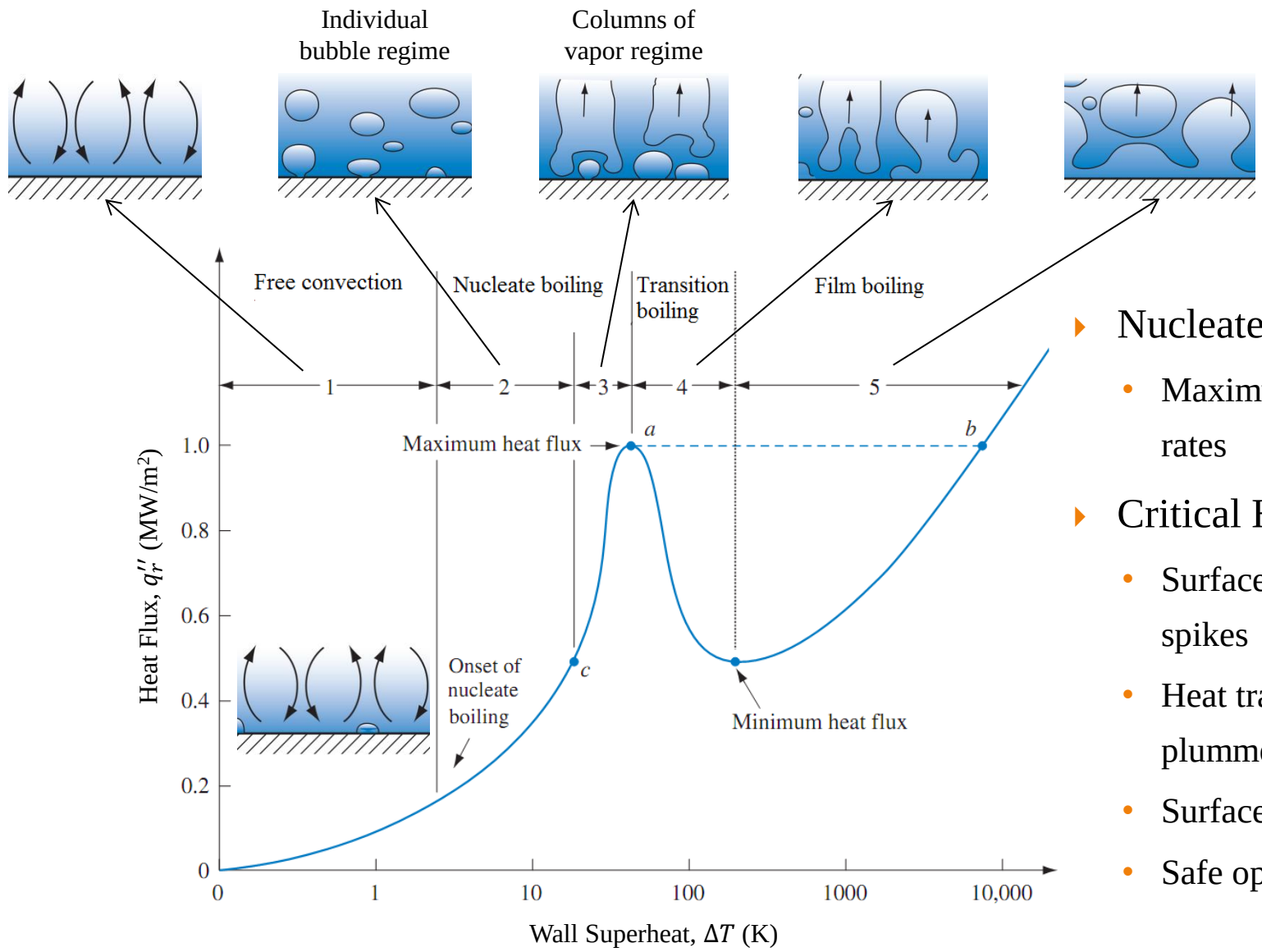

- Nucleate boiling regime
  - Maximum heat transfer rates
- Critical Heat Flux
  - Surface temperature spikes
  - Heat transfer rate plummets
  - Surface or system failure
  - Safe operating conditions

Literature Review

- Pool boiling over cylindrical tube surfaces
  - Single tube systems
  - Surface modifications
    - Passively enhances the heat transfer performance and system efficiencies
- Bubble dynamics over modified surface
- Surface modifications techniques broadly categorized as:
  - Open microchannels/Integral fins
  - Re-entrant cavities
  - Porous surfaces

Open Microchannels/Integral Fins

Cooke and Kandlikar (2012) *[32]*

- Working fluid: Distilled water
- Enhancement technique:
  - Open microchannels over flat surfaces
- Performance enhancement effects of microchannel geometric parameters
- Enhancement factor:
  - High heat fluxes: 3.7
- Achieved a record heat transfer coefficient of 269 kW/m^2·K, at a heat flux of 2440 kW/m^2

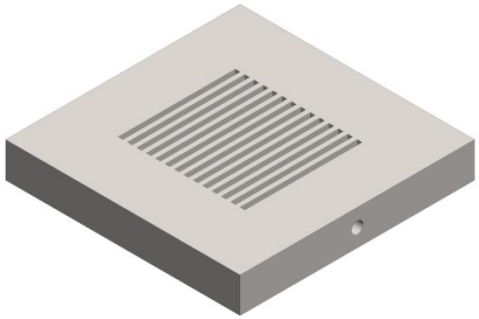

Open microchannel surface

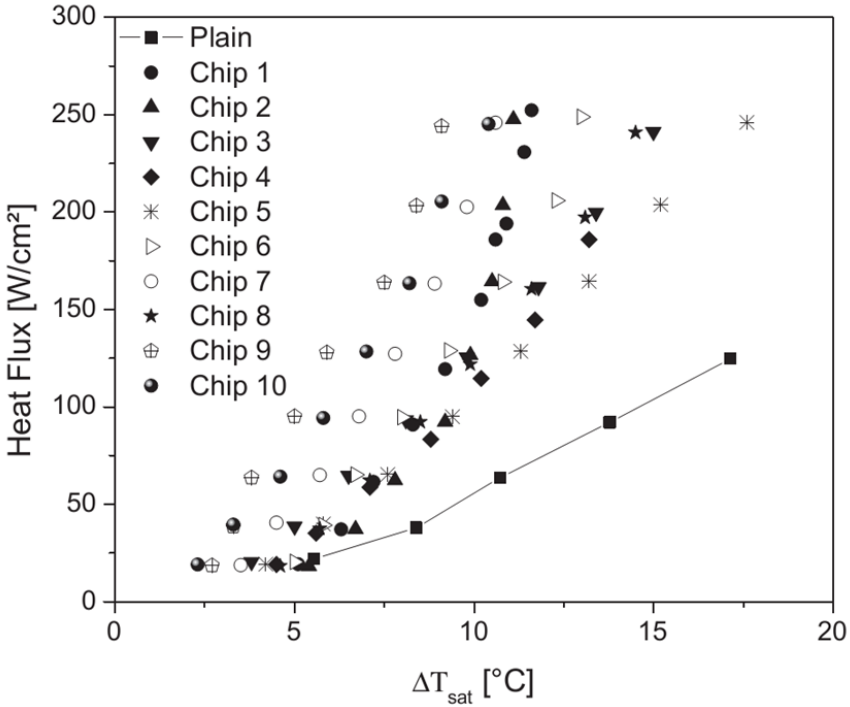

Boiling curves for different geometries

Open Microchannels/Integral Fins

Saidi et al. (1999) *[30]*

- Working fluid: R123
- Enhancement technique:
  - High and low density microchannel surfaces
- Enhancement factors:
  - High fin density: 2.2 – 2.4
  - Low fin density: 1.3 – 2.4
- Observed steady enhancement over the entire heat flux range

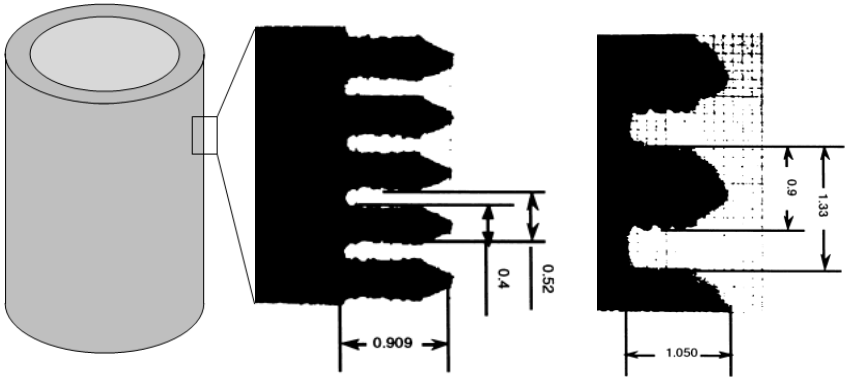

High and low fin density tube surfaces

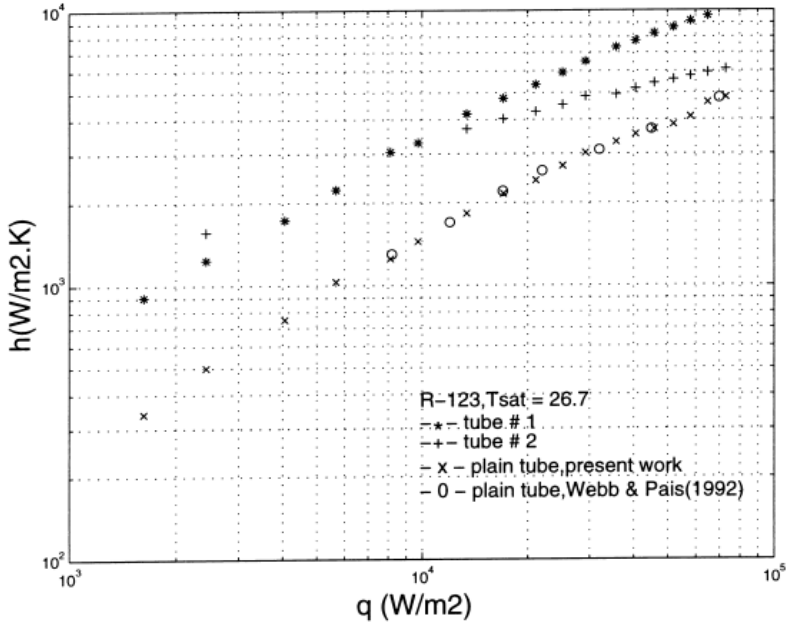

Performance comparison for enhanced tubes

Re-entrant Cavities

Memory et al. (1995) *[4]*

- Working fluid: R114
- Enhancement technique:
  - GEWA T19, T26, YX26, Thermoexcel-HE, and Turbo-B
- Enhancement factors:
  - Low heat fluxes: 5.5
  - High heat fluxes: 3
- Steady drop in performance with increase in heat flux conditions

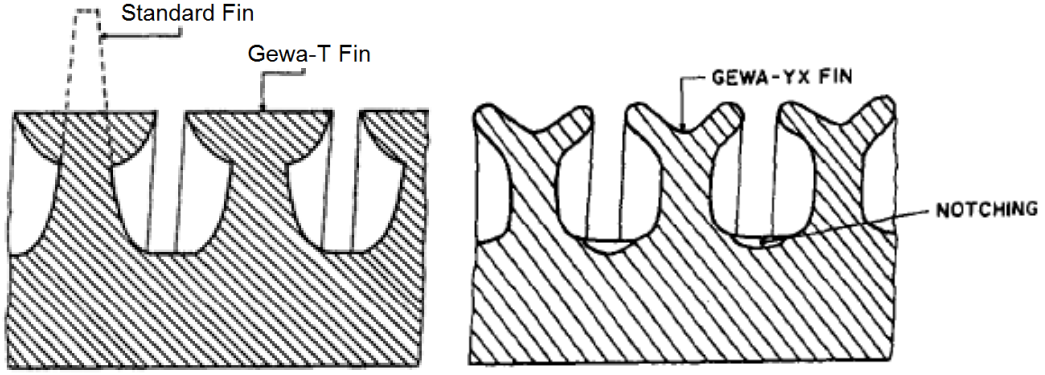

GEWA-T and YX re-entrant cavity structures

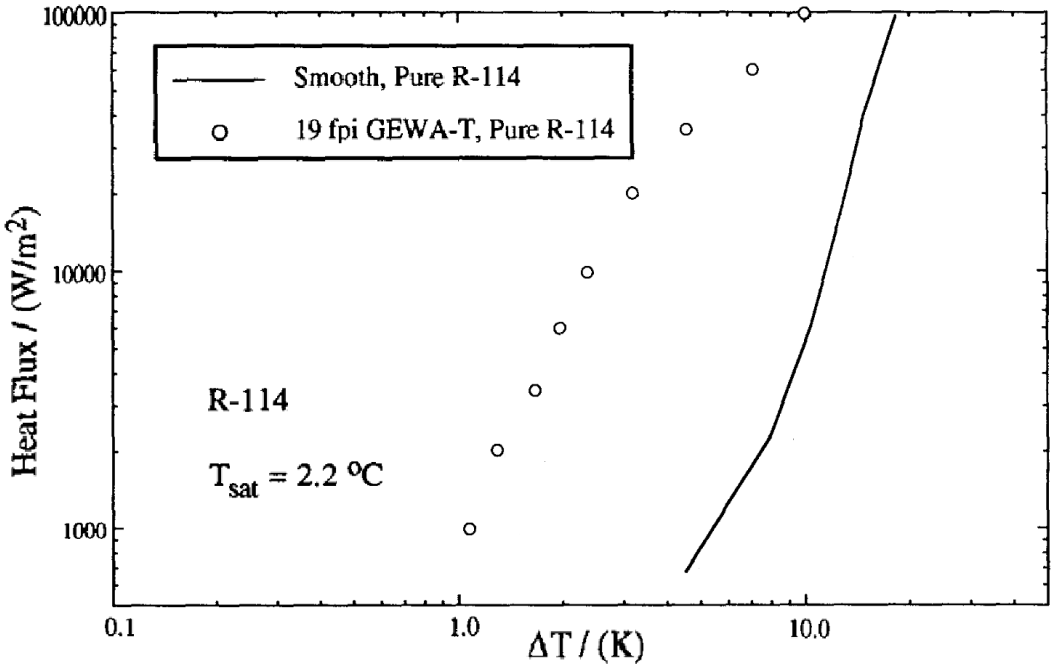

Performance of GEWA-T19 tube with pure R114

Re-entrant Cavities

Chien and Webb (1998) *[12-14]*

- Working fluid: Methanol
- Enhancement technique:
  - Pored foil over finned tubes
- Preferred dimensions
  - Greater tunnel height
  - Smaller tunnel pitch
- Sharp corners aided in nucleation
- 10 – 20% increased performance in the horizontal orientation

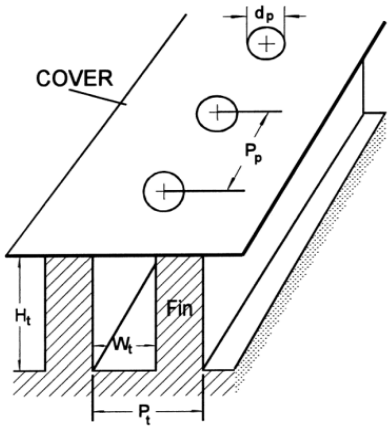

H_t – tunnel height
W_t – tunnel width
P_t – tunnel pitch
P_p – pore pitch
d_p – pore diameter

Schematic of porous foil on a finned tube

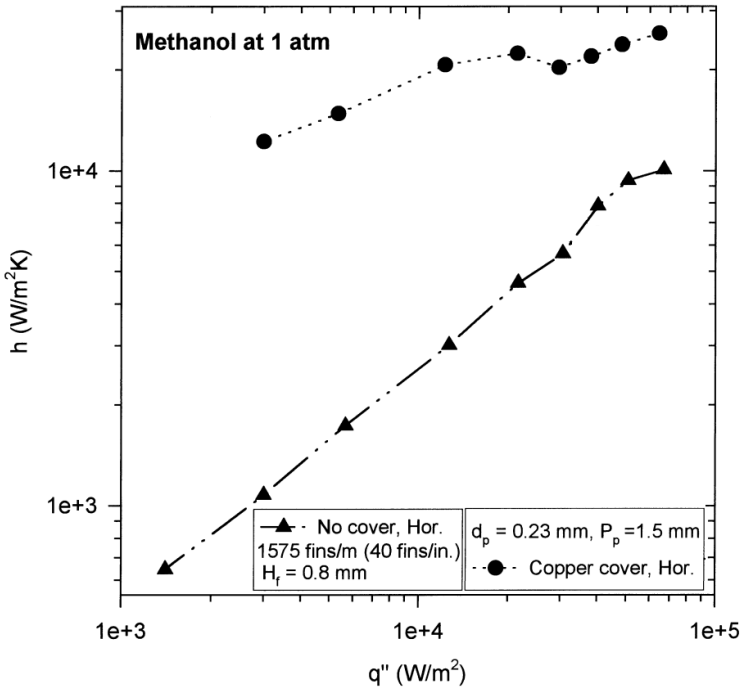

Experimental results copper cover surface

Porous Surfaces

Cieslinski (2002) [24]

- Working fluid: Distilled water
- Enhancement technique:
  - Metal porous layer deposited surfaces
- Parametric study of coatings over stainless steel tubes
  - Coating materials: Al, Cu, Zn, Brass, and Mo
- Onset of nucleate boiling at 0.1 K wall superheats
- Best performance enhancement with Al coating
- Observed “in-coating crisis”

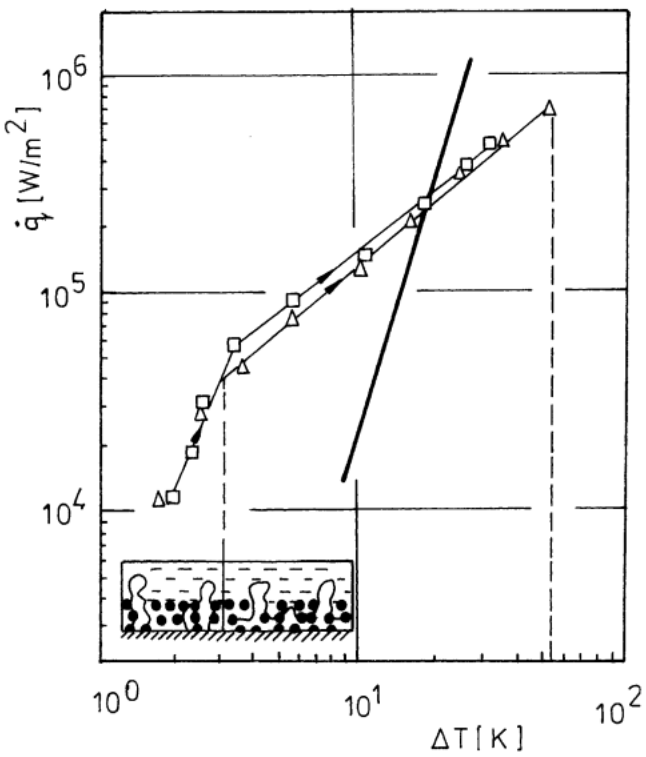

Performance curves for Al porous coating tube and smooth tube, showing “in-coating crisis”

Porous Surfaces

Ribatski and Thome (2006) *[10]*

- Working fluid: R134a
- Enhancement technique:
  - HIGHFLUX tube
- Enhancement factors:
  - Low heat fluxes: 21.3
  - High heat fluxes: 4.9
- Significant drop in performance enhancements at high heat flux conditions

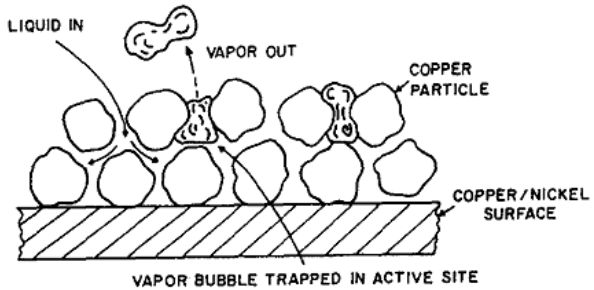

Porous HIGHFLUX tube surface [4]

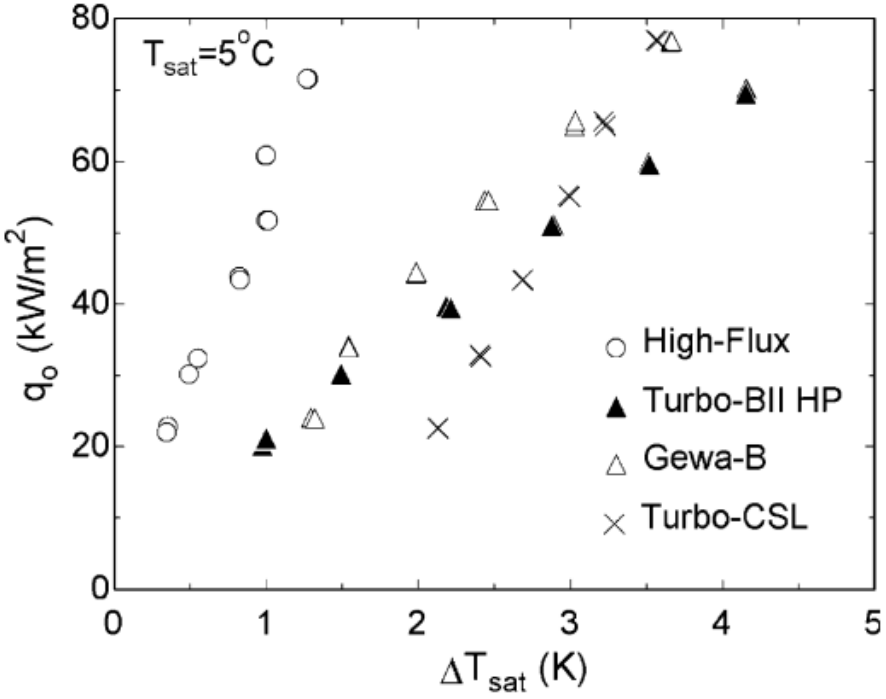

Boiling curves for enhanced tubes under decreasing heat flux conditions

Bubble Dynamics

Chien and Webb (1998) [12-14]

- Visualized boiling process in the sub-surface tunnels
  - Evaporation mechanism
  - Bubble emergence from pores
- Rectangular and circular fin bases

- Observed mostly vapor filled tunnels
- Liquid meniscus in the rectangular base channel corners
- Aided replenish the working fluid

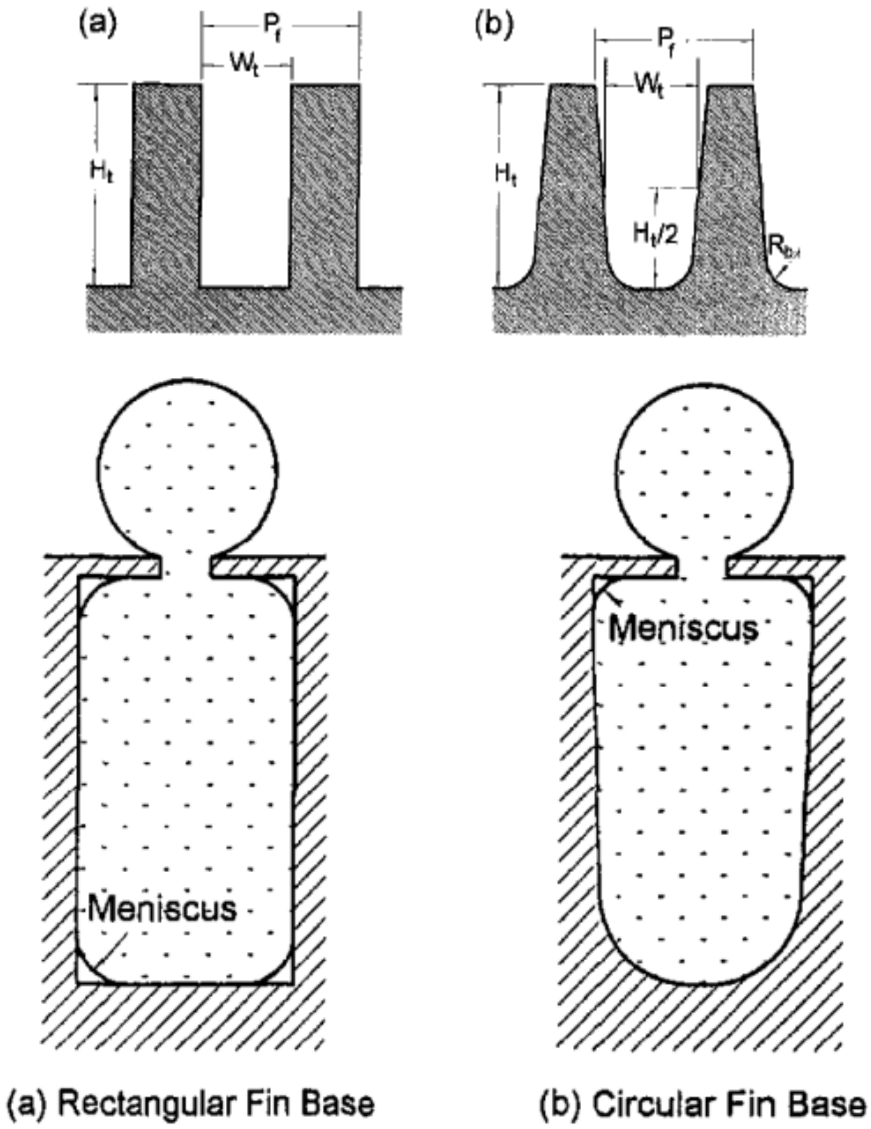

Tunnel cross-section

Bubble Dynamics

Cooke and Kandlikar (2011) *[31]*

- Bubble growth on top surface of the microchannel walls
- Microchannels remain flooded
  - Providing pathway for the working fluid
  - Lowering wall superheat
- Rewetting phenomenon responsible for superior performance

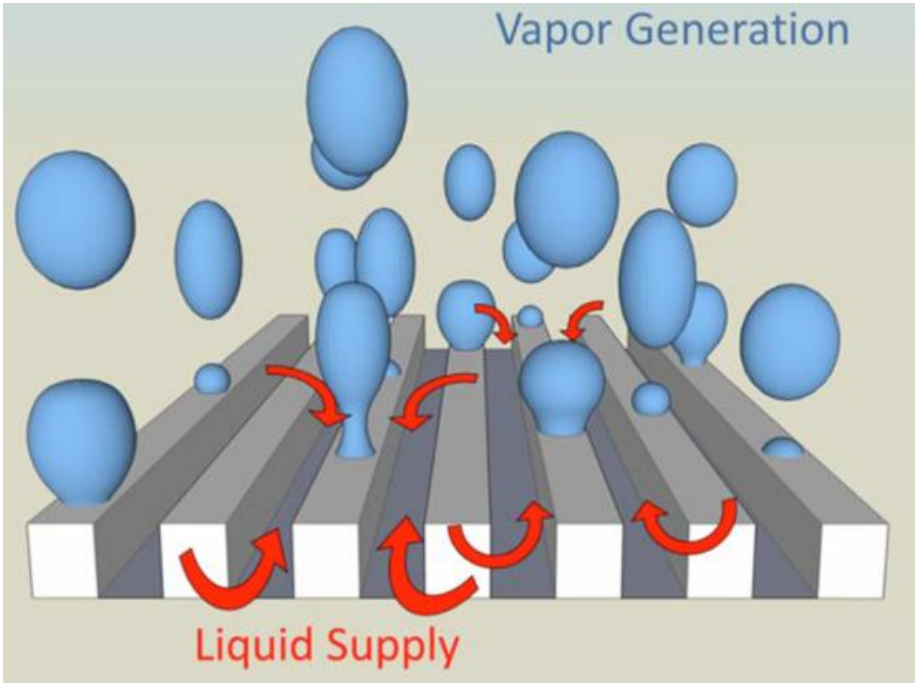

Proposed bubble dynamics mechanism

Literature Review: Summary

- Re-entrant cavity and porous surface tubes
  - Significantly high heat transfer enhancements were observed at low heat flux conditions
  - Sharp drop in the performance enhancement factors with an increase in the heat flux conditions
- Open microchannels over flat and cylindrical surfaces showed significant enhancements in the heat transfer performance
- Surface modifications on the cylindrical tubes were only circumferentially oriented
- An increase in the overall performance of the surface was observed in the horizontal orientation
- Microchannel grooves and sharp corners aided in the rewetting of the heated surface

Objectives

- Enhance heat transfer performance
  - Over cylindrical tubes
  - Under high heat flux conditions
- Improve the Critical Heat Flux limit
  - To extend safe operating limits for a system and enhance its efficiency
- Study the bubble behavior over microchannel surfaces
  - To reveal and comprehend the underlying fundamental heat transfer mechanisms

Approach

- Design an experimental setup to investigate pool boiling at high heat flux conditions

- Develop microchannel surfaces over cylindrical tubes
- Conduct a parametric study to analyze the effects of:
  - Microchannel orientation
  - Cross-section geometries
  - Dimension of the geometric parameters
  - Tube orientation

- Visualize the bubble interactions over the microchannel surfaces
  - Videography using high-speed microscope camera

Design of Experimental Setup

- Test in horizontal and vertical orientations
- Working fluid: Distilled water
- Peripheral systems and equipment
  - TDK-Lambda power supplies
    - 3.3 kW and 1.5 kW
  - Auxiliary heater from Watlow®
    - 200 W @ 120 V
  - Data acquisition systems and sensors

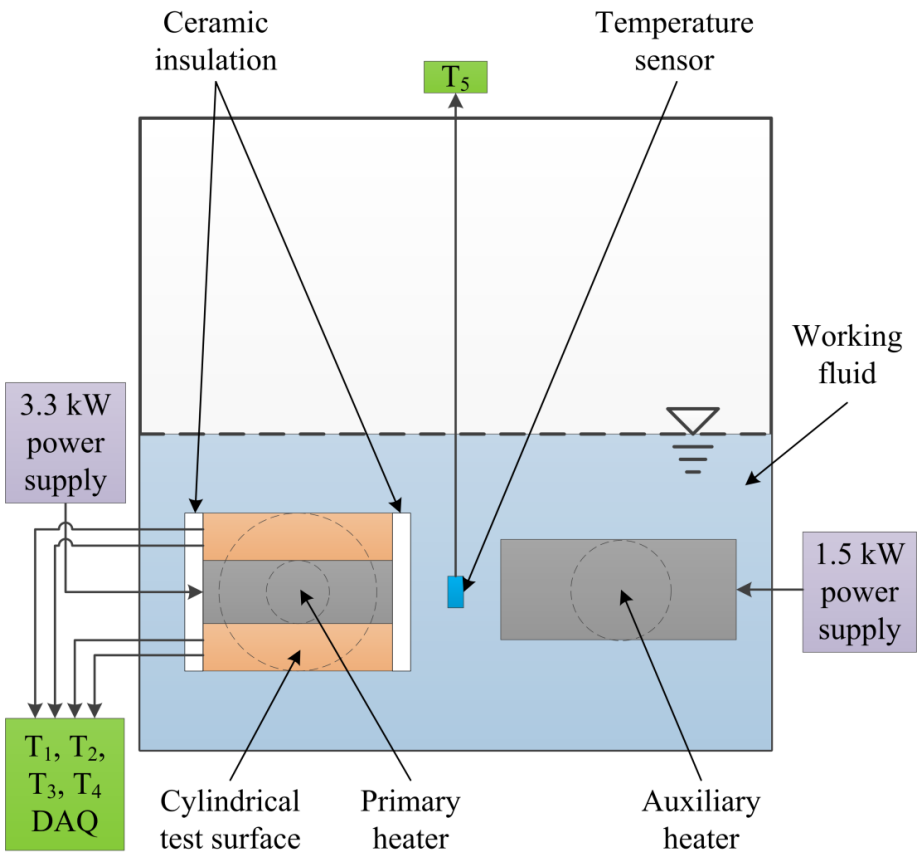

System schematic
with test section in the horizontal orientation

Design of Test Section Assembly

- Primary heater
  - Yielded 1000 W @ 190 V
    - Rated for 400 W @ 120 V
  - Delivering up to 1100 kW/m^2
    - Test section outer surface
- Maximize radial heat transfer
  - Thermal compound (Artic Silver®)
- Minimize axial heat losses
  - Thermally insulating ceramic spacers
- Setup was axially compressed
  - Top and bottom plates
  - Gaskets

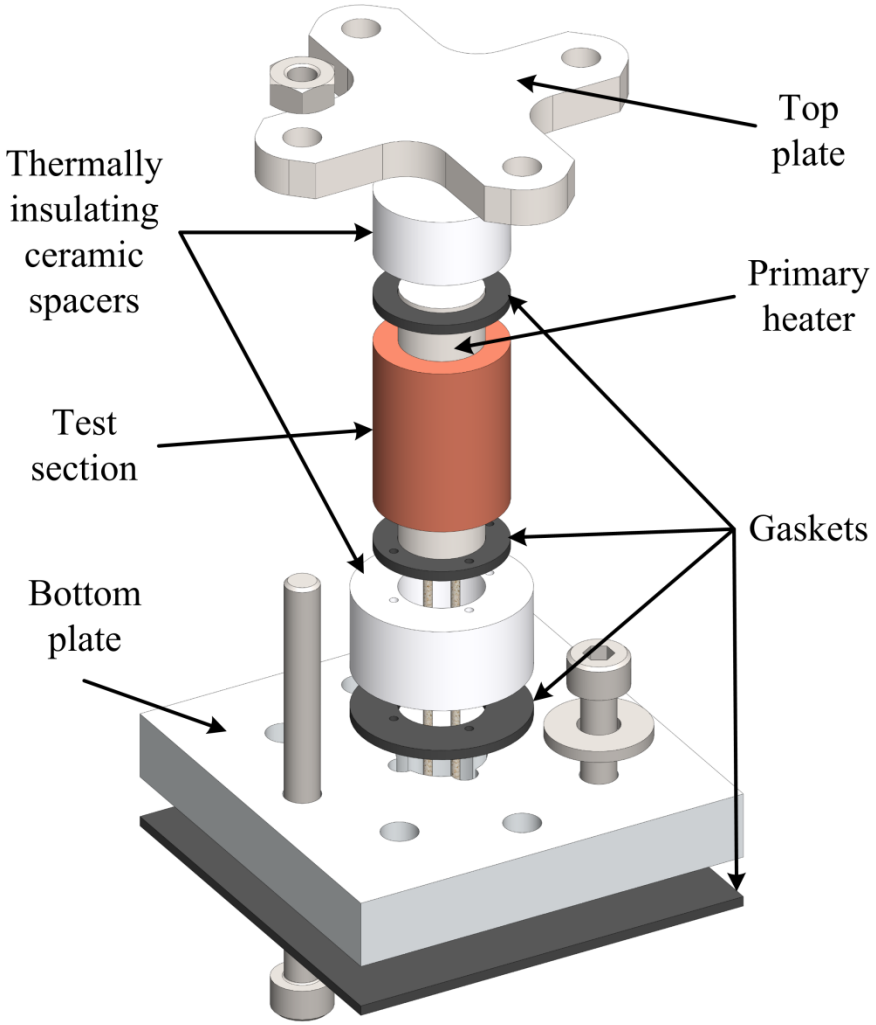

Exploded view of test section assembly

Design of Test Surfaces

Plain Test Section (P0)

- Material: Copper alloy 101
  - Thermal conductivity, $k = 391$ W/m·K
- Design based on primary heater size
- Microchannels machined on the outer surface

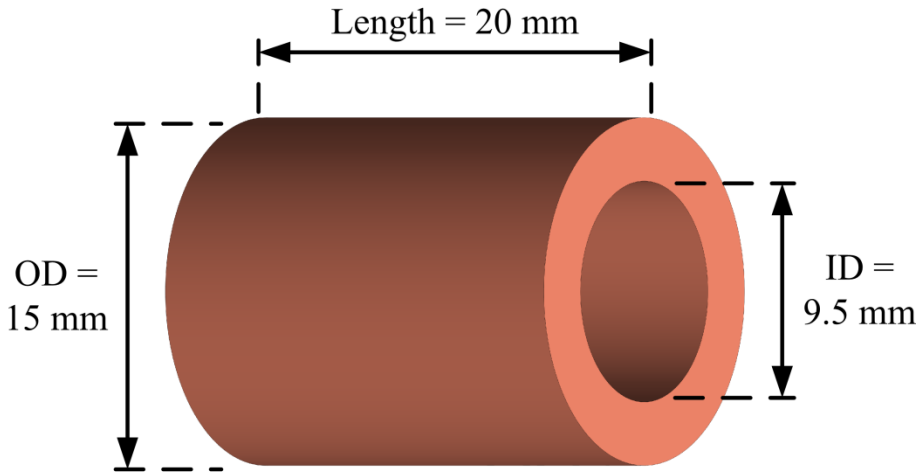

Plain test section dimensions

Microchannel Orientations

- Circumferential around the test section
- Axially along the length of the test section

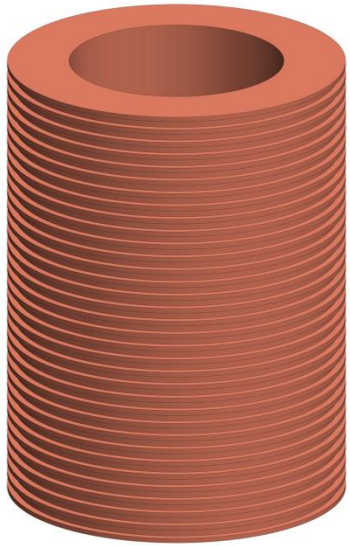

Circumferential

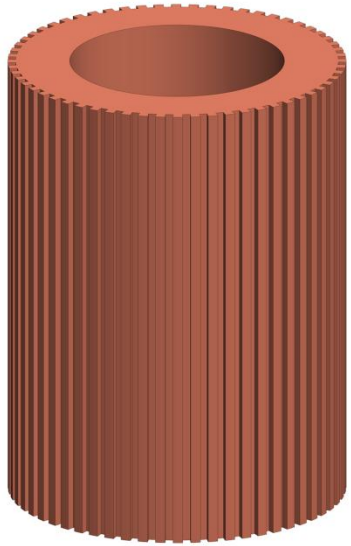

Axial

Details of Cross-section Geometries and Test Sections

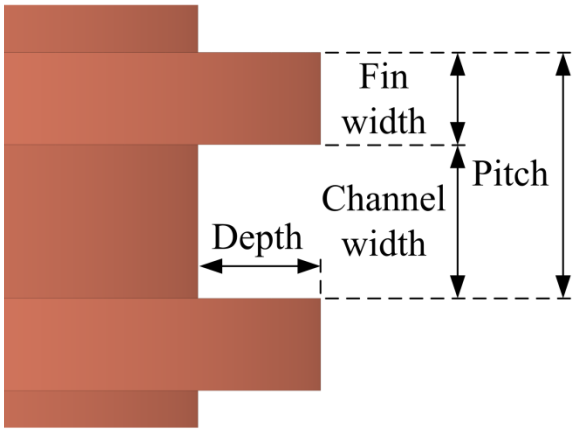

Circumferential **Rectangular** Microchannels (CRM)

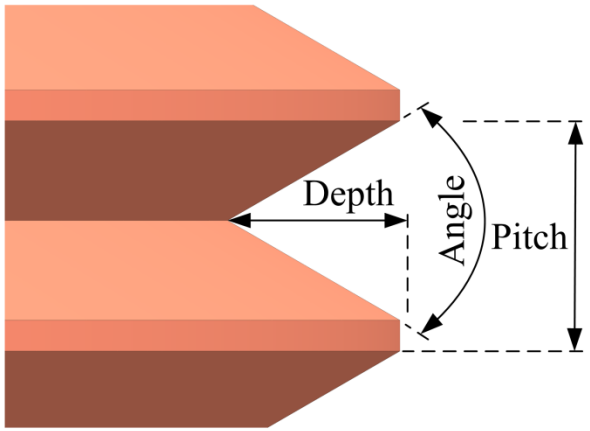

Circumferential **V-groove** Microchannels (CVM)

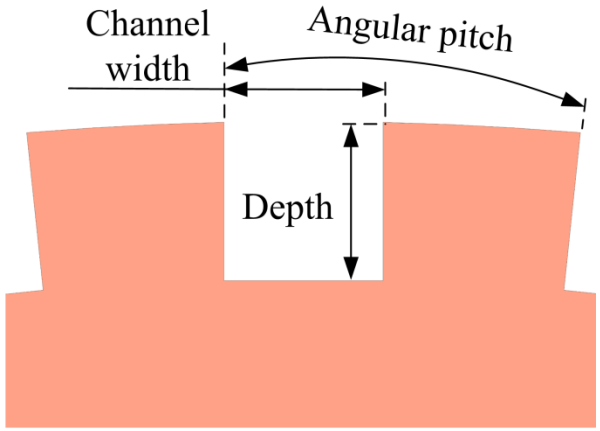

Axial **Rectangular** Microchannels (ARM)

- Developed twenty unique test sections by varying:
  - Microchannel orientation
  - Cross-section geometries
  - Dimension of the geometric parameters
- Verified the dimensions using a Confocal Laser Scanning Microscope (CLSM)
- $$Area\ Enhancement\ Factor = \frac{Total\ wetted\ surface\ area\ for\ the\ microchannel\ test\ section}{Total\ wetted\ surface\ area\ for\ the\ plain\ test\ section}$$

Test Section Matrix

Test Section	*Depth* (mm)	*Pitch* (mm) / (°)	*Channel Width* (mm)	*Fin Width* (mm)	*Included Angle* (°)	*Area Enhance-ment Factor*
P0	-	-	-	-	-	1.00
CRM1	**0.29**	**0.59**	**0.38**	**0.21**	-	1.95
CRM2	0.38	0.59	0.36	0.23	-	2.18
CRM3	0.25	0.70	0.38	0.32	-	1.67
CRM4	0.41	0.70	0.40	0.30	-	2.06
CRM5	**0.30**	**0.50**	**0.29**	**0.21**	-	2.13
CRM6	0.37	0.50	0.28	0.22	-	2.40
CRM7	**0.26**	**0.60**	**0.30**	**0.30**	-	1.80
CRM8	**0.36**	**0.59**	**0.30**	**0.29**	-	2.11
CVM1	0.24	0.39	-	-	60	1.68
CVM2	0.31	0.55	-	-	60	1.60
CVM3	0.37	0.54	-	-	60	1.74
CVM4	0.43	0.70	-	-	60	1.65
CVM5	0.32	0.40	-	-	45	2.03
CVM6	0.46	0.55	-	-	45	2.03
ARM1	**0.22**	**6**	**0.40**	-	-	1.57
ARM2	**0.39**	**6**	**0.40**	-	-	1.95
ARM3	0.22	6	0.52	-	-	1.56
ARM4	0.22	8	0.54	-	-	1.42
ARM5	0.37	8	0.53	-	-	1.71
ARM6	0.51	8	0.53	-	-	1.95

CLSM Analysis

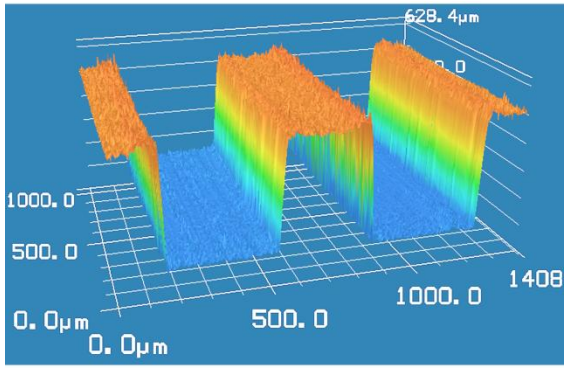

3D surface profile for CRM4

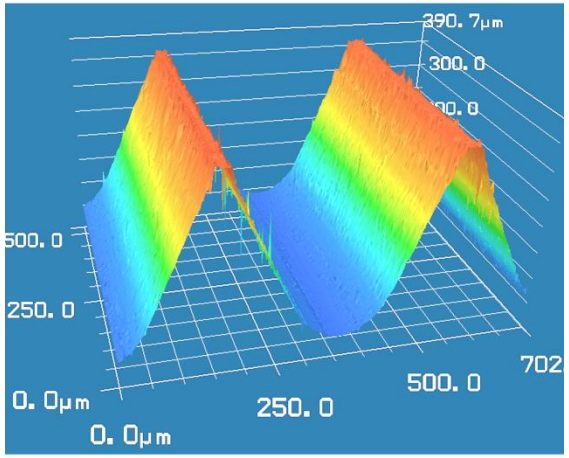

3D surface profile for CVM5

Data Acquisition

- USB chassis: NI cDAQ-9172
- Temperature module: NI-9213
- T-type thermocouples from OMEGA
  - 0.8 mm sheathed and grounded probes
  - 4 thermocouples: $T_1 - T_4$
    - Measures the temperatures inside the test section
    - Located radially, at a depth of 10 mm
  - 5th thermocouple: T_5
    - Measure the bulk fluid temperature
- LabVIEW™ custom VI
  - Manually recorded: Voltage, V and current, I
  - Data logging rate: 5 Hz for 20 seconds
  - Indicated whether steady state conditions were attained

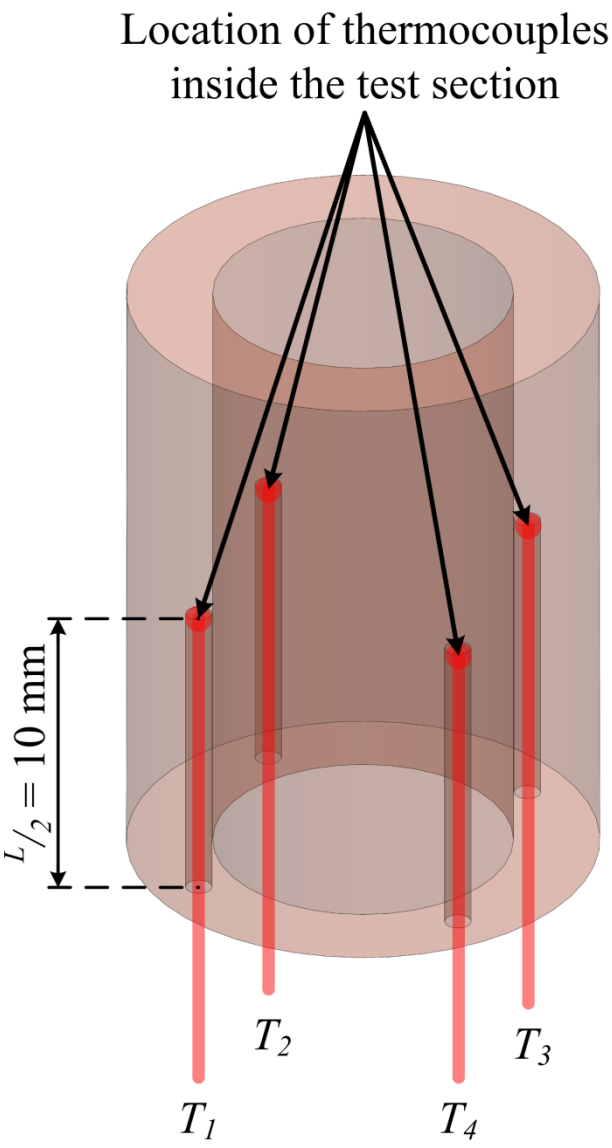

Data Reduction

- Total heat input:

$$q_h = V \times I$$

- Axial heat losses: $q_{a,l}$
  - Numerical study showed losses < 2%
- Resultant radial heat output:

$$q_r = q_h - q_{a,l}$$

- Average temperature @ r_1:

$$T_{ave} = \frac{T_1 + T_2 + T_3 + T_4}{4}$$

- Surface temperature @ r_2:

$$T_s = T_{ave} - \left(q_r \times \frac{\ln(r_2/r_1)}{2\,\pi\,k\,L} \right)$$

- Resultant radial heat flux at outer diameter:

$$q_r'' = \frac{q_r}{A_s}$$

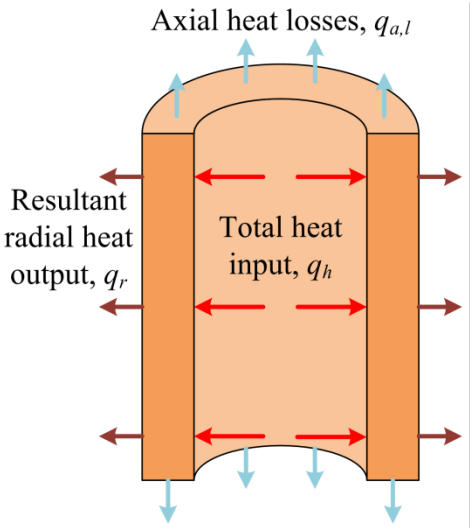

Heat input and output surfaces

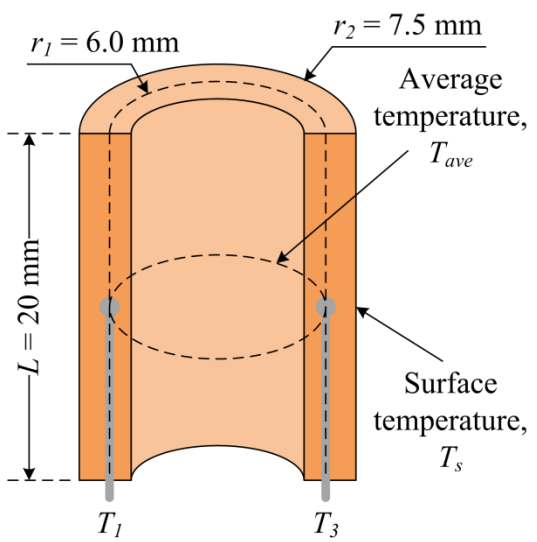

Radii for average and surface temperatures

- Heat transfer coefficient:

$$h = \frac{q_r''}{(T_s - T_5)}$$

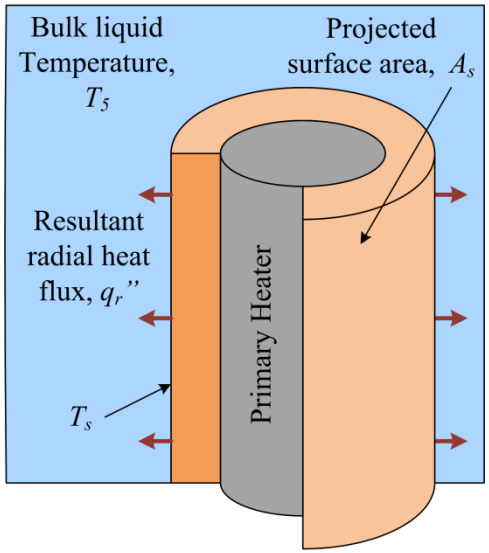

Experimental Procedure

- Working fluid: Distilled water
  - Saturation temperature = 100°C
- Power supplied
  - Primary and auxiliary heaters
- Degassing of water
- Heat flux condition
  - Adjusting the voltage across the heater
- Data logged after attaining steady state conditions:
  - Test section (fluctuations < ±0.1°C)
  - Working fluid ($T_5 \cong T_{saturation}$)

- Step-wise increasing and decreasing heat flux conditions
- Tube Orientations:
  - Horizontal and vertical

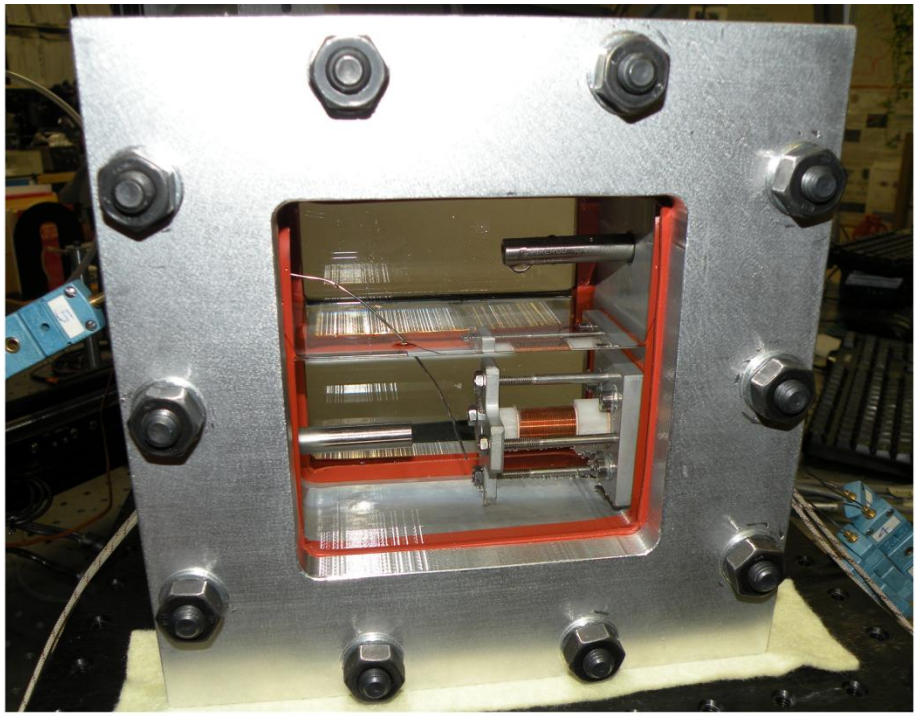

Picture of assembled experimental setup

Results and Discussions

Plain Test Section Experimental Results

- Critical Heat Flux (—): P0
  - $q''_{CHF} \cong 700$ kW/m^2
- Maximum heat flux (- -):
  - $q''_{max} = 667$ kW/m^2
- Horizontal orientation
  - Heat transfer coefficient, $h = 38$ kW/m^2·K
    - $\Delta T = 17.8$ K
- Vertical orientation
  - Heat transfer coefficient, $h = 36$ kW/m^2·K
    - $\Delta T = 18.8$ K

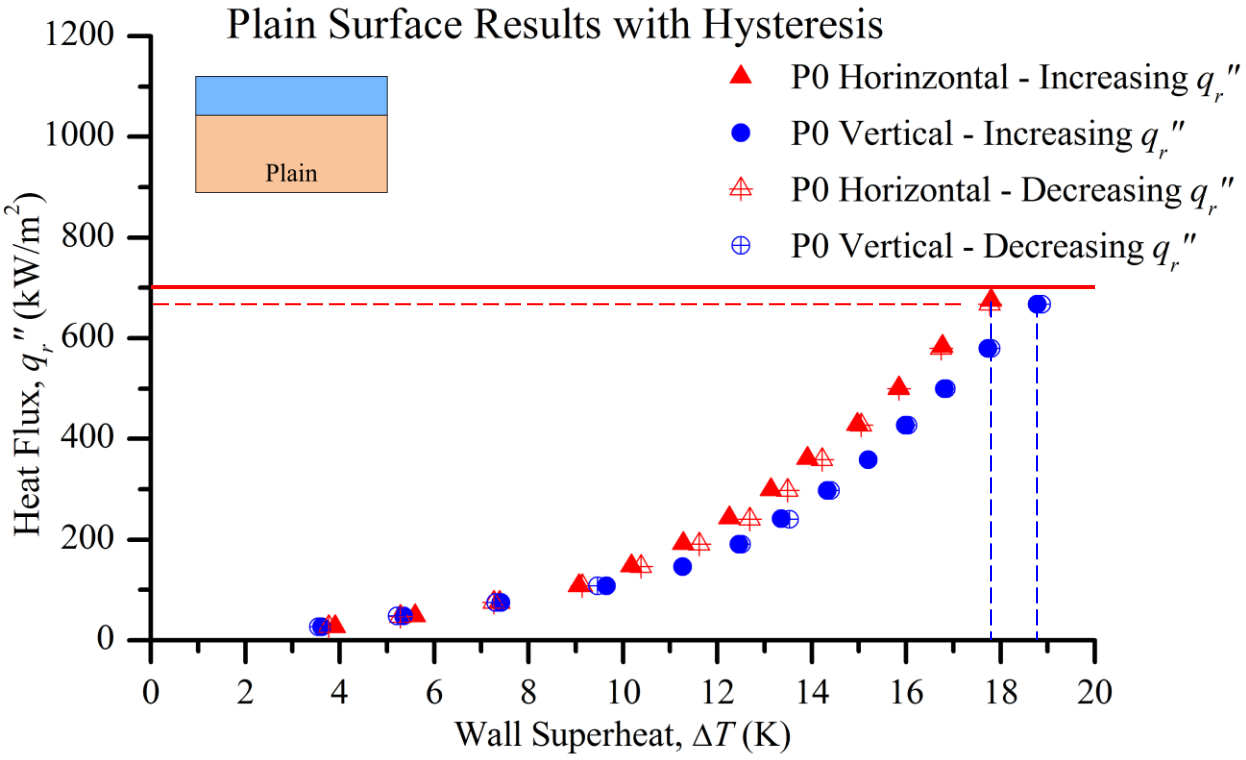

- Negligible hysteresis for all test sections
  - In horizontal and vertical orientations

CRM Experimental Results

Horizontal Orientation Results

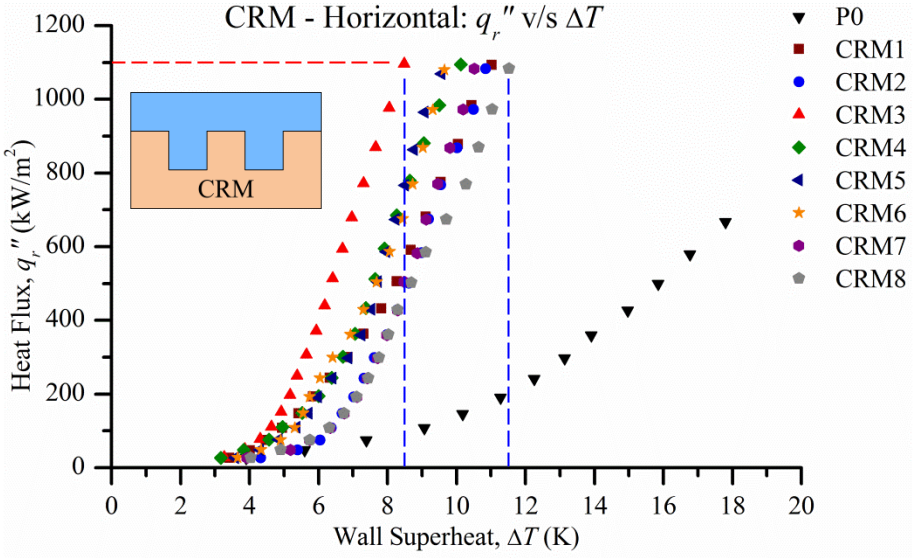

Vertical Orientation Results

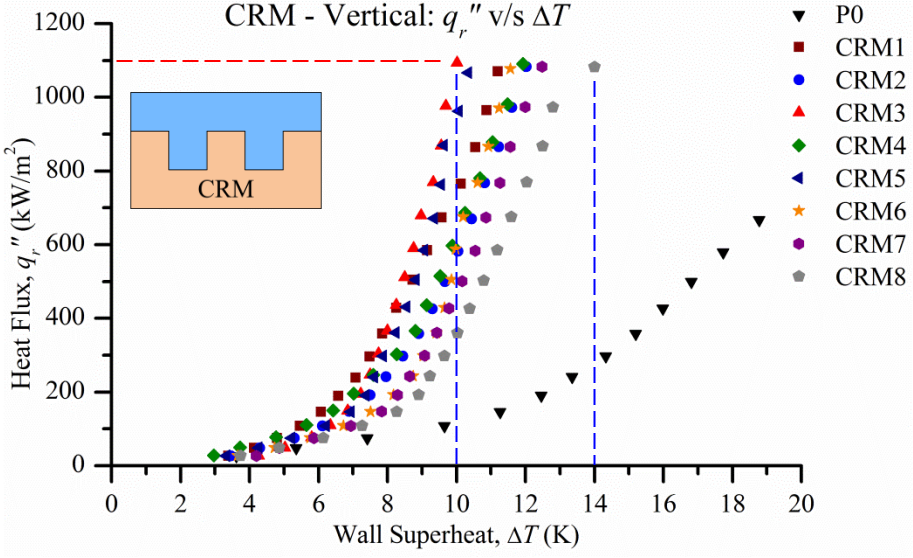

- $q''_{max} \cong 1100$ kW/m^2 (heater limited)
- None of the CRM test sections reached CHF limits (either orientations)
- Significant heat transfer performance enhancements were achieved
- Better performance in the horizontal orientation

CRM Heat Transfer Performance

- Highest achieved heat transfer coefficient (- -): CRM3
  $h = \mathbf{129\ kW/m^2{\cdot}K}$
  - $\Delta T = \mathbf{8.5\ K}$
  - $q''_{max} = 1095\ \text{kW/m}^2$
- Uncertainty in h for CRM3
  - At highest heat flux condition: **±7.9%**

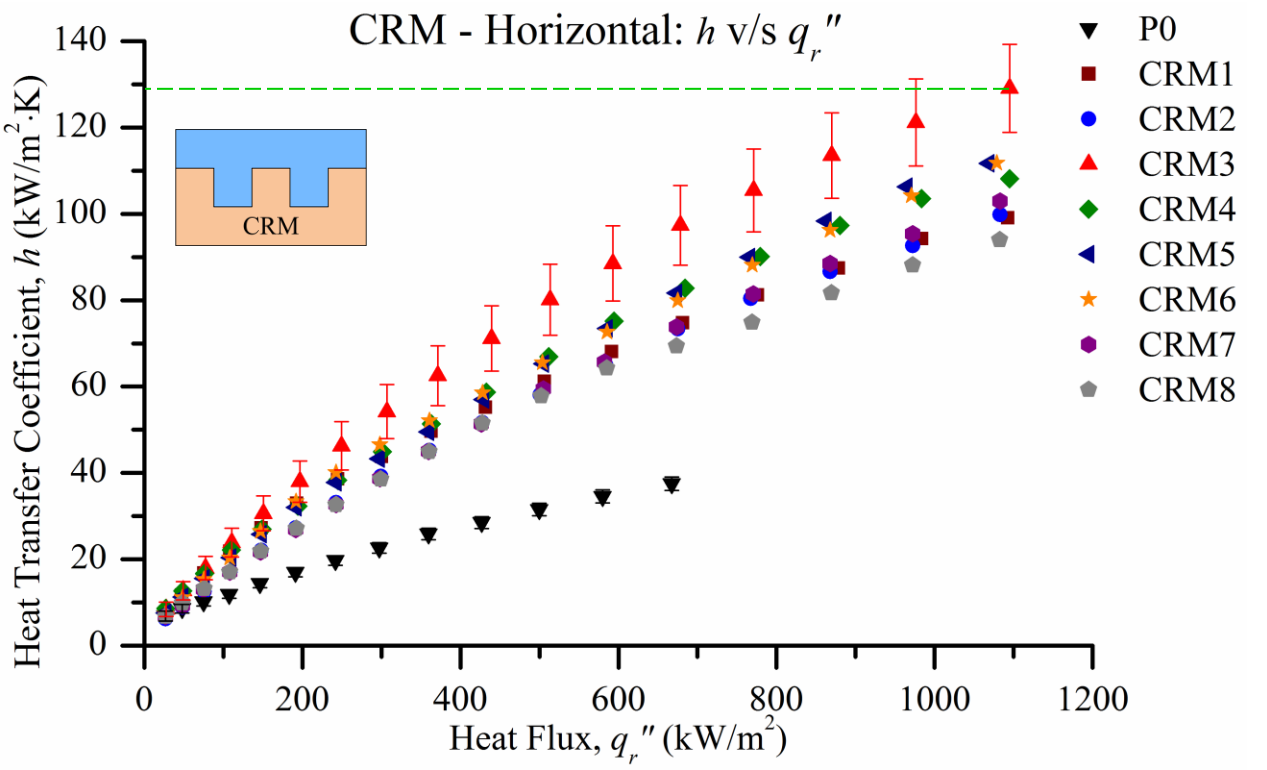

- Steady increase in heat transfer coefficients with an increase in the heat flux conditions

Overall Enhancements in Heat Transfer Performance

- Horizontal orientation enhancement factors: 2.5 – **3.4**
- Vertical orientation enhancement factors: 2.2 – **3.1**
- CHF improvement factor: **1.6**
  - $q''_{CHF,P0} \cong 700$ kW/m^2 to $q''_{max,CRM} = 1100$ kW/m^2

Test Section	*Horizontal Orientation*				*Vertical Orientation*			
	q''_{max} kW/m^2	ΔT K	h kW/m^2·K	h_{CRM}/h_{P0} -	q''_{max} kW/m^2	ΔT K	h kW/m^2·K	h_{CRM}/h_{P0} -
P0	667.3	17.8	37.5	-	667.2	18.8	35.5	-
CRM1	1092.9	11.0	99.1	2.6	1070.7	11.2	95.6	2.7
CRM2	1082.9	10.9	99.8	2.7	1082.7	12.0	90.0	2.5
CRM3	**1095.2**	**8.5**	**129.1**	**3.4**	**1093.0**	**10.0**	**109.1**	**3.1**
CRM4	1095.0	10.1	108.1	2.9	1090.8	11.9	91.4	2.6
CRM5	1068.9	9.6	111.7	3.0	1066.8	10.3	103.2	2.9
CRM6	1079.0	9.7	111.7	3.0	1076.7	11.6	93.1	2.6
CRM7	1082.9	10.5	103.0	2.8	1082.6	12.5	86.7	2.4
CRM8	1082.7	11.5	94.0	2.5	1082.4	14.0	77.3	2.2

Effects of Channel Depth

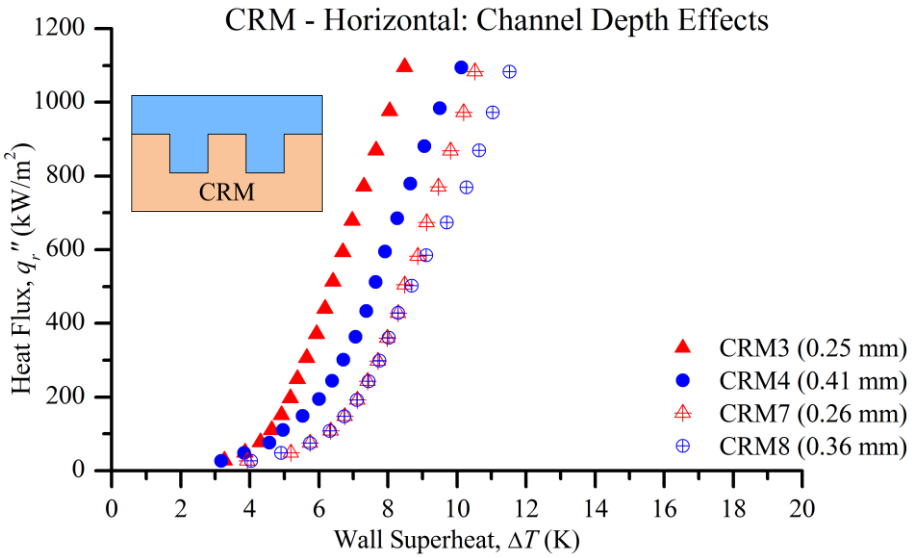

- Channel depth range:
  - 0.25 – 0.41 mm
- Shallower microchannel depths
  - Yield superior heat transfer performances

Effects of Channel Width

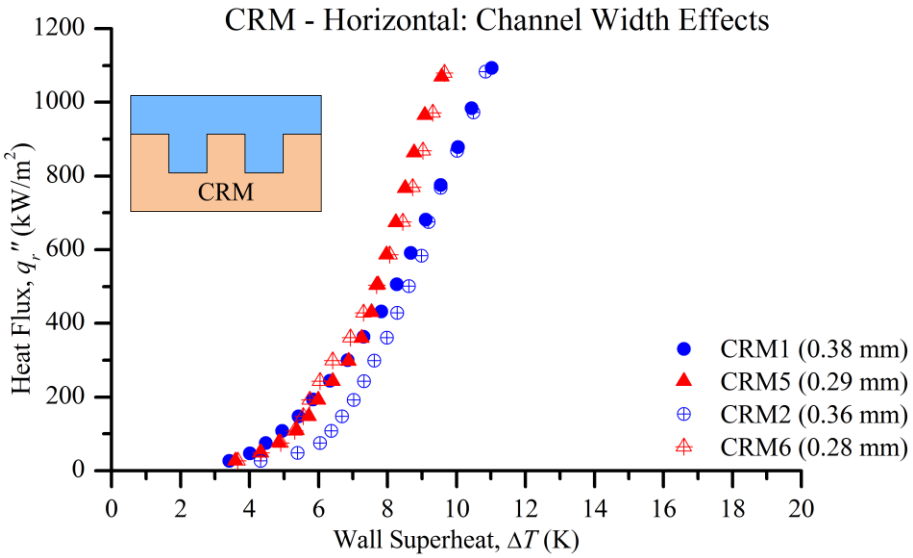

- Channel width range:
  - 0.28 – 0.40 mm
- Narrower microchannels
  - Shows better performance
- Effect primarily at high heat fluxes

Effects of Fin Width

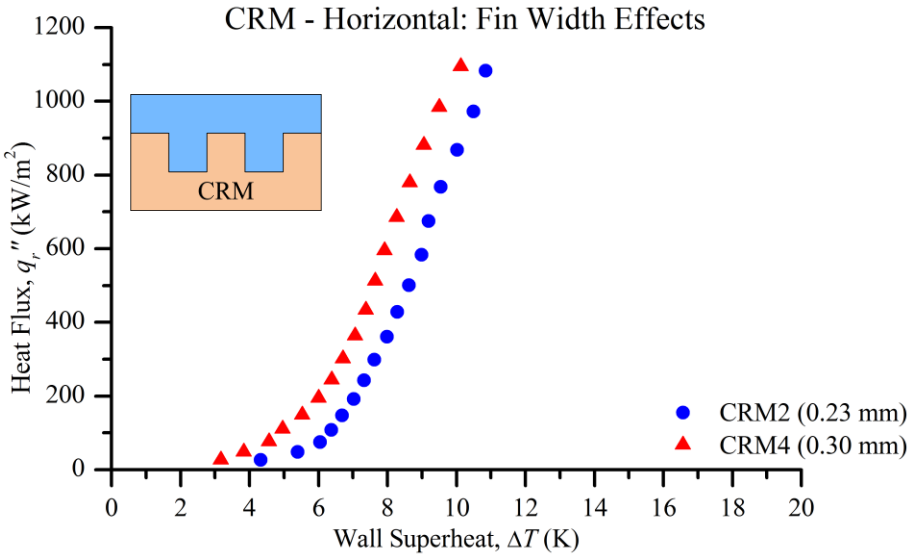

- Fin width range:
  - 0.21 – 0.32 mm
- Wider fins
  - Yield better heat transfer performance

Area Normalized Results

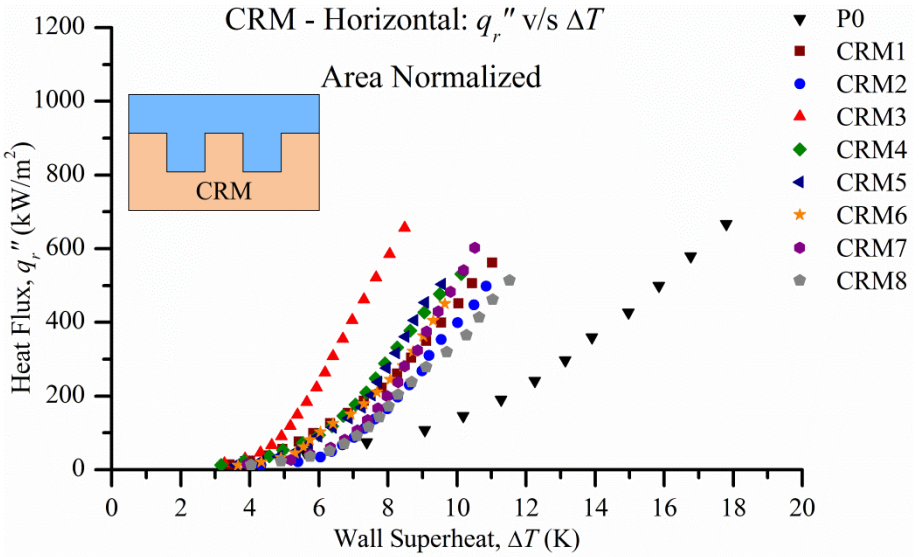

- Re-evaluated heat fluxes
  - Total wetted surface area
- Factors other than area augmentation responsible for performance enhancement

CVM Experimental Results

Horizontal Orientation Results

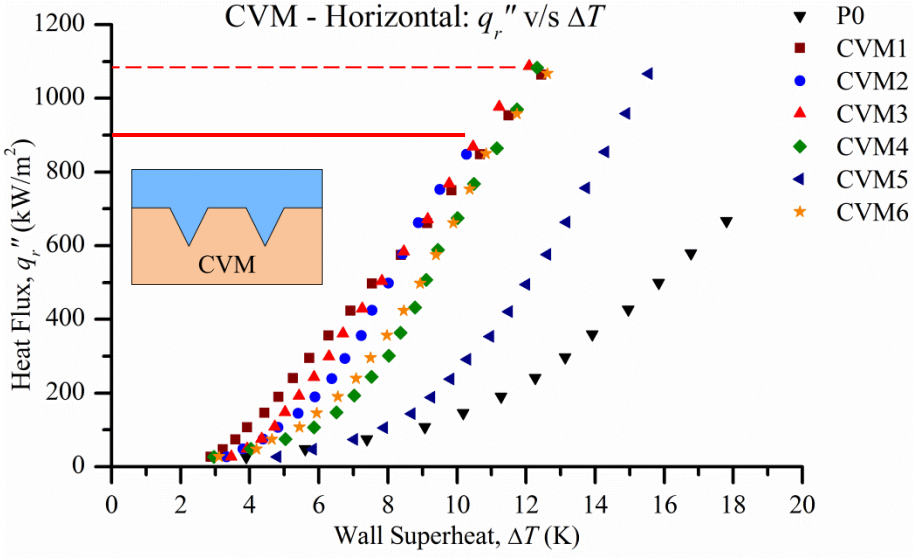

- $q''_{max} \cong 1070$ kW/m^2 (heater limited)
- Insignificant effect of the geometric parameters on the boiling curves
- Critical Heat Flux: CVM2
  - $q''_{CHF} \cong 900$ kW/m^2

Area Normalized Results

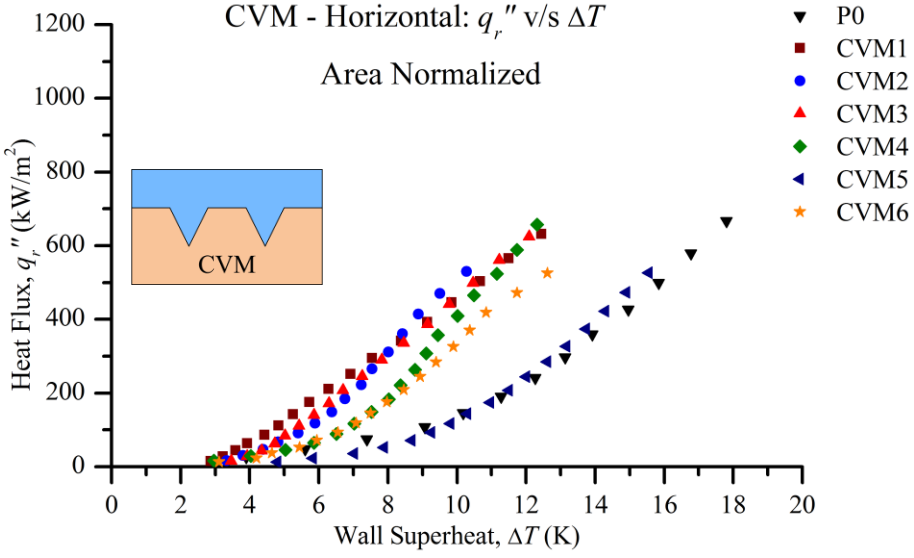

- CVM5's poor performance
  - Sharp and narrow 45° included angle
  - Low channel pitch
  - Shallow grooves
- Similar to P0's performance

Overall Enhancements in Heat Transfer Performance

- Horizontal orientation enhancement factors: 1.8 – **2.4**
- Vertical orientation enhancement factors: 2.0 – **2.3**
- CHF improvement factor (except CVM2): **1.5**
  - $q''_{CHF,P0} \cong 700$ kW/m^2 to $q''_{max,CVM} = 1070$ kW/m^2

Test Section	*Horizontal Orientation*				*Vertical Orientation*			
	q''_{max} kW/m^2	ΔT K	h kW/m^2·K	h_{CVM}/h_{P0} -	q''_{max} kW/m^2	ΔT K	h kW/m^2·K	h_{CVM}/h_{P0} -
P0	667.3	17.8	37.5	-	667.2	18.8	35.5	-
CVM1	1064.5	12.5	85.5	2.3	1066.2	14.5	73.7	2.1
CVM2	**847.9**	**10.3**	**82.5**	**2.2**	966.4	11.8	81.6	2.3
CVM3	1086.7	12.1	89.9	2.4	1086.4	14.3	76.1	2.1
CVM4	1082.6	12.3	87.8	2.3	1082.4	14.0	77.3	2.2
CVM5	1066.0	15.6	68.5	1.8	1066.1	14.9	71.5	2.0
CVM6	1066.5	12.6	84.5	2.3	1066.4	13.1	81.7	2.3

ARM Experimental Results

Vertical Orientation Results

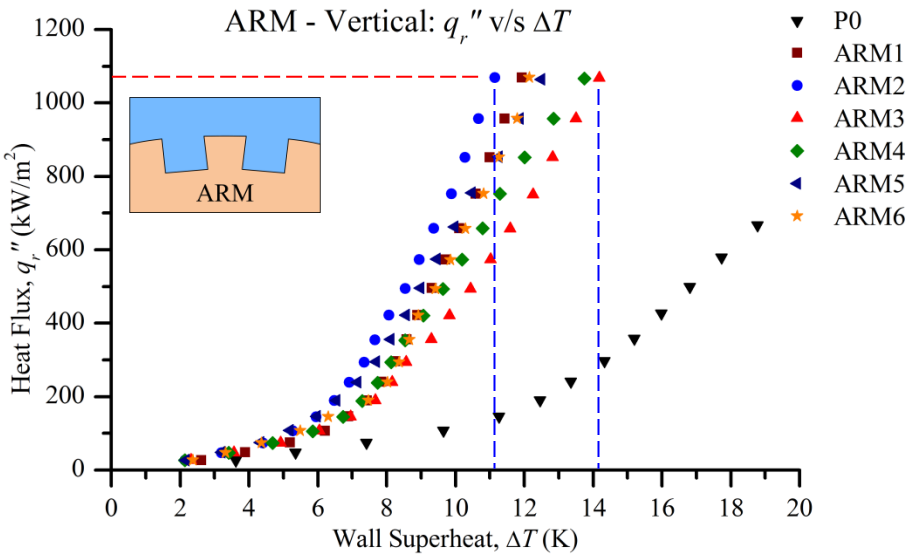

Horizontal Orientation Results

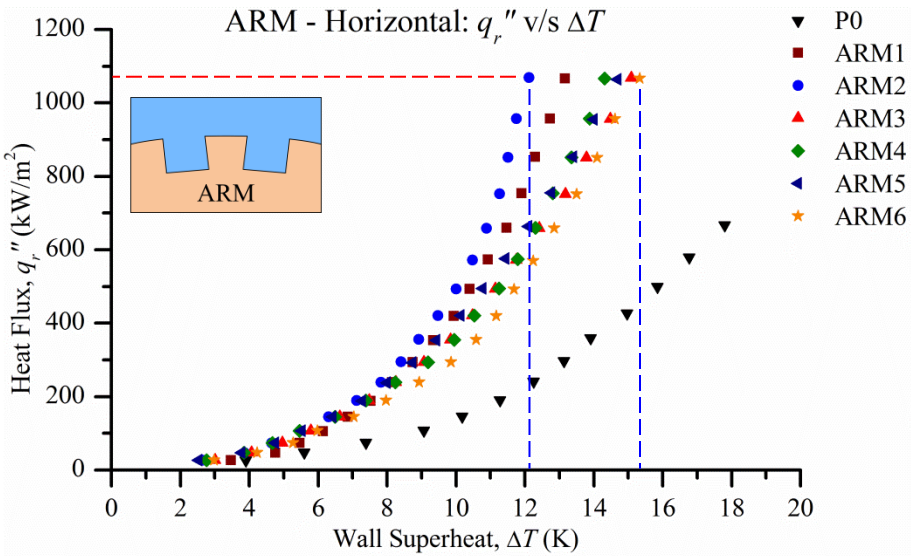

- $q''_{max} \cong 1070$ kW/m^2 (heater limited)
- None of the ARM test sections reached CHF limits (either orientations)
- Good heat transfer performance enhancements were observed
- Better performance in vertical orientation

ARM Heat Transfer Performance

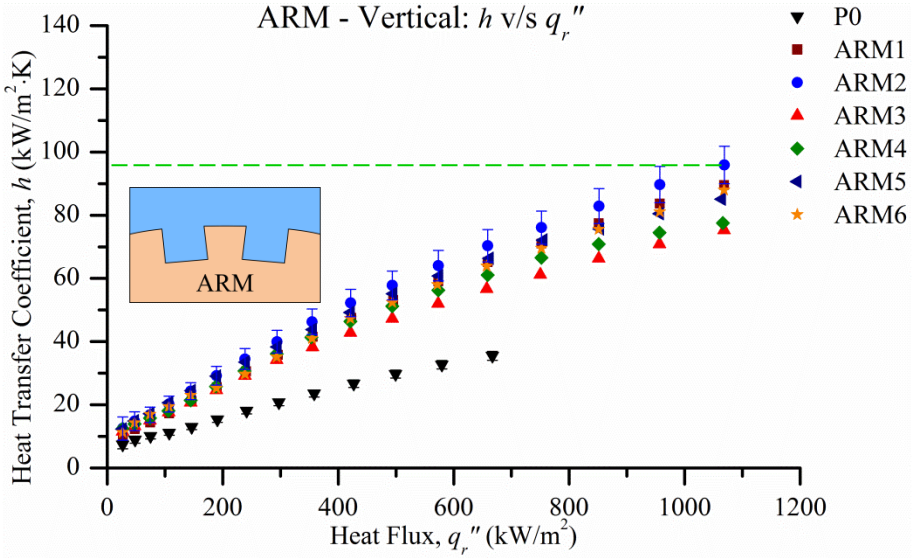

- Heat transfer coefficient: ARM2

  h = **96 kW/m²·K**
  - ΔT = **11.1 K**
  - q''_{max} = 1069 kW/m²
- Uncertainty in h for ARM2
  - At highest heat flux condition: **±6.2%**

Area Normalized Results

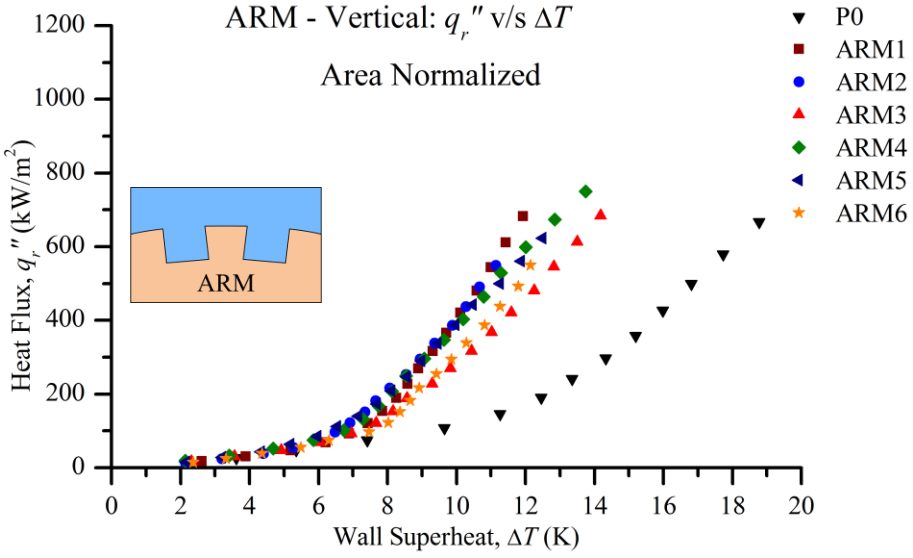

- Good performance enhancements were observed with all ARM surfaces
- Rectangular cross-section grooves show significant enhancements for the circumferentially and axially oriented microchannels

Overall Enhancements in Heat Transfer Performance

- Vertical orientation enhancement factors: 2.1 – **2.7**
- Horizontal orientation enhancement factors: 1.9 – **2.3**
- CHF improvement factor: **1.5**
  - $q''_{CHF,P0} \cong 700$ kW/m^2 to $q''_{max,ARM} = 1070$ kW/m^2

Test Section	*Horizontal Orientation*				*Vertical Orientation*			
	q''_{max} kW/m^2	ΔT K	h kW/m^2·K	h_{ARM}/h_{P0} -	q''_{max} kW/m^2	ΔT K	h kW/m^2·K	h_{ARM}/h_{P0} -
P0	667.3	17.8	37.5	-	667.2	18.8	35.5	-
ARM1	1066.4	13.2	81.0	2.2	1068.6	11.9	89.5	2.5
ARM2	1068.5	12.1	88.1	2.3	**1068.7**	**11.1**	**95.9**	**2.7**
ARM3	1068.1	15.1	70.8	1.9	1068.2	14.2	75.3	2.1
ARM4	1066.2	14.3	74.4	2.0	1066.3	13.8	77.5	2.2
ARM5	1064.1	14.7	72.4	1.9	1064.4	12.5	85.1	2.4
ARM6	1066.1	15.3	69.5	1.9	1068.5	12.1	88.0	2.5

Effects of Channel Depth

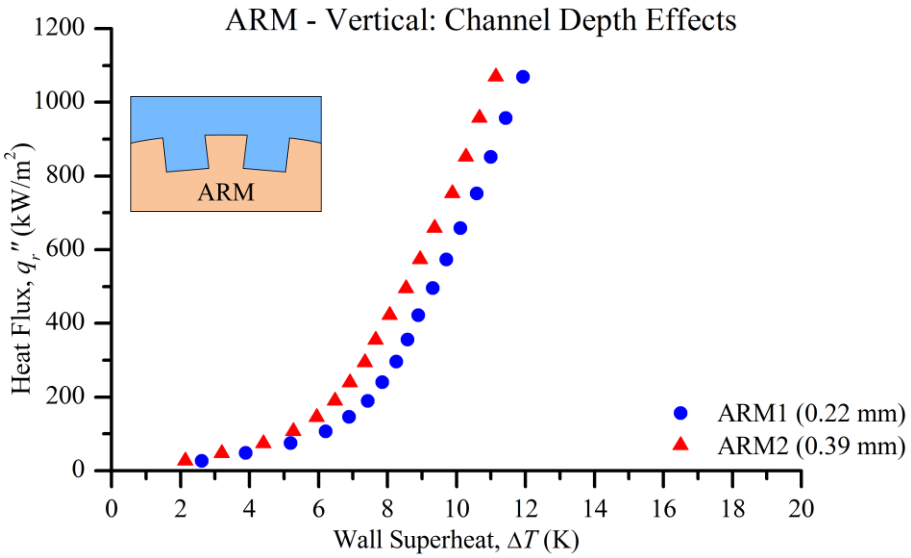

- Channel depth range:
  - 0.22 – 0.51 mm
- Deeper microchannels
  - Yield better heat transfer performance

Effects of Channel Width

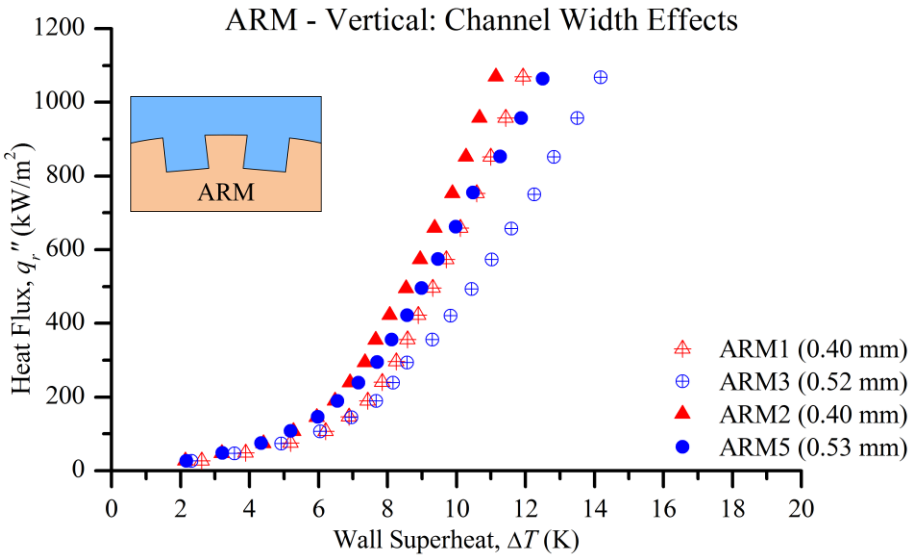

- Channel width range:
  - 0.40 – 0.54 mm
- Narrower microchannels
  - Delivers better performance
- Effect primarily at high heat fluxes

Effects of Tube Orientation

- Circumferentially grooved, CRM and CVM test sections
  - Yield better performances in horizontal orientation
  - **10 – 20%** greater performance

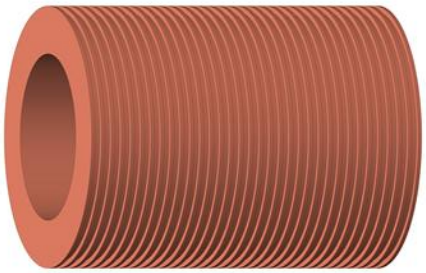

- Axially grooved, ARM test sections
  - Yield better performances in vertical orientation
  - **10 – 15%** greater performance

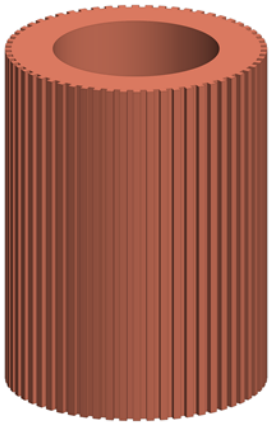

- Tube orientation performance enhancement
  - Depends on the orientation of the microchannels

Bubble Dynamics

Setup and Details

- High-speed microscope camera
- Recording conditions
  - 50X magnification
  - 1000 or 4000 fps
    - Better analyze bubble movement
- Only circumferentially grooved test surfaces
  - V-groove cross-section
  - Rectangular cross-section
- Mainly in the low heat flux range
  - Generate uninterrupted and clear videos

Low Heat Flux Condition

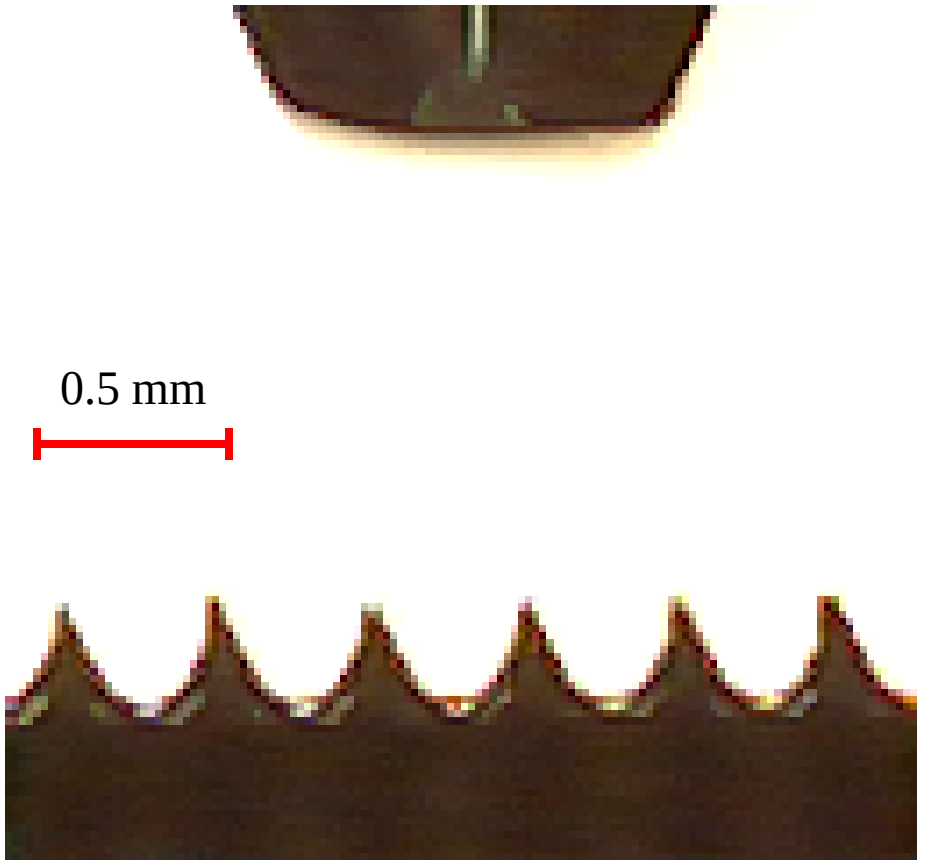

Top surface of CVM1 at low heat flux

Medium Heat Flux Condition

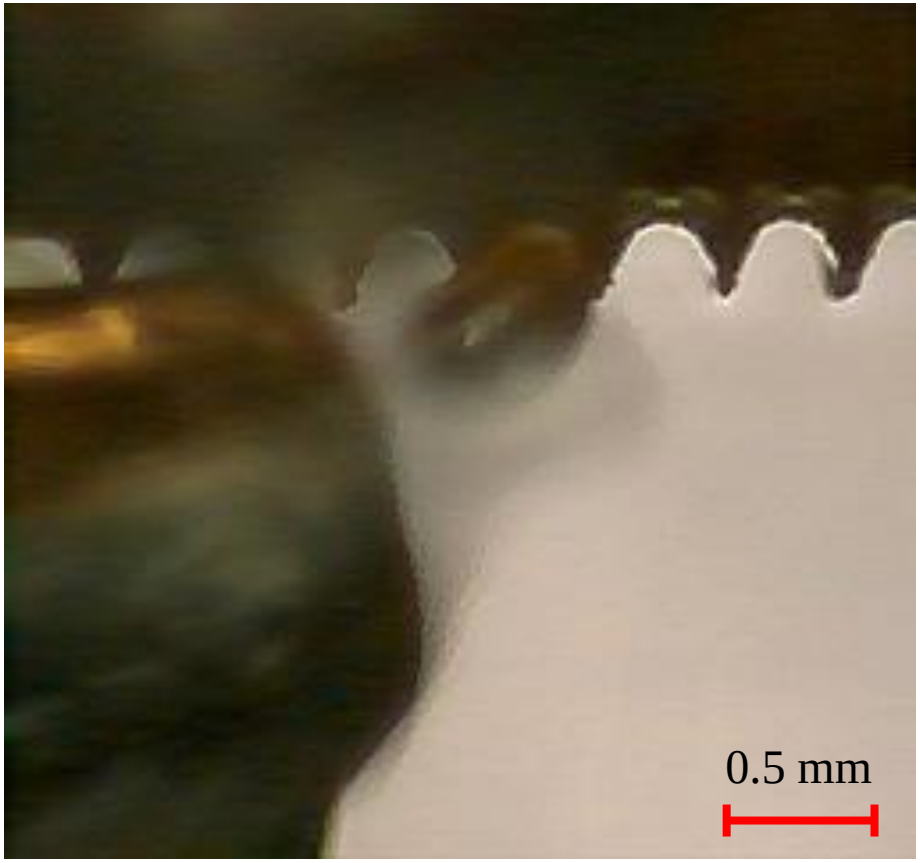

Bottom surface of CVM1
at a heat flux of 75 kW/m^2

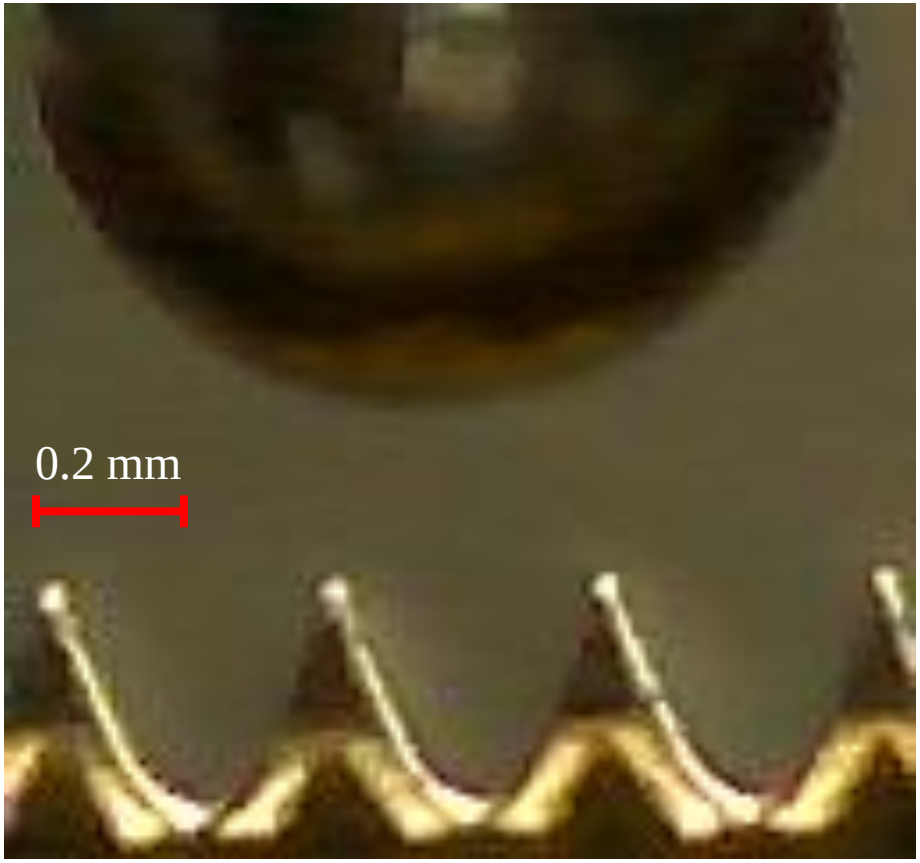

Top surface of CVM5
at a heat flux of 80 kW/m^2

High Heat Flux Condition

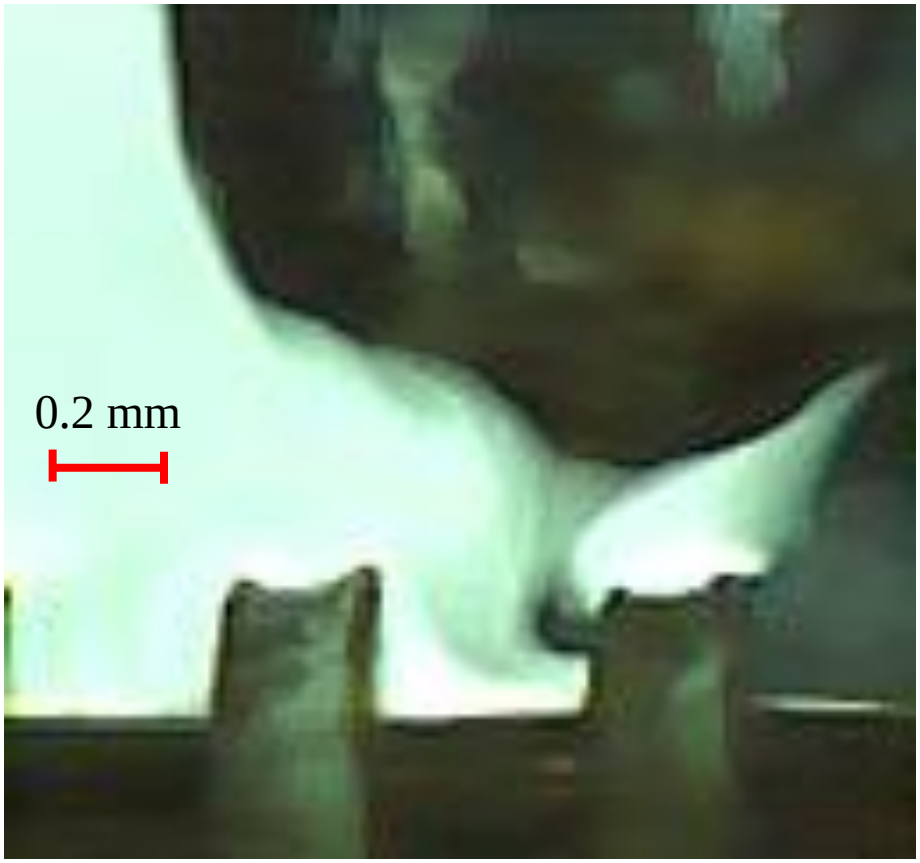

Top surface of CRM3
at a heat flux of 150 kW/m^2

- Low heat flux conditions
  - Individual bubble nucleation
  - Low bubble generation rates
- Medium heat flux conditions
  - Bubble feeding mechanism
  - Alternate nucleation of nearby cavities
- High heat flux conditions
  - Higher bubble generation rates
  - Simultaneous nucleation of numerous cavities
  - Multiple bubble feeding mechanisms in close proximity

- Instantaneous bubble ejection from grooves
- Completely vapor filled V-grooves
- Liquid filled corners with rectangular cross-section geometry channels

Conclusions

- Significant heat transfer performance enhancement
  - With microchannel surfaces over plain surfaces
- Greatest heat transfer enhancement factor of **3.4** was achieved with CRM3
  - Highest heat transfer coefficient of **129 kW/m^2·K** and a wall superheat of **8.5 K**
- Extension in the critical heat flux limit
  - By a factor of at least **1.6** over the plain surface CHF limit
- Influence of geometric parameters on overall performance
  - CRM: Narrower, and shallower microchannels with wider fins
  - CVM: Insignificant effects of geometric parameters
  - ARM: Narrower, and deeper microchannels

Conclusions

- Tube orientation preferentially enhanced heat transfer performance
  - Horizontal orientation favored circumferentially grooved test sections
  - Vertical orientation favored axially grooved test sections
- Cross-section geometries
  - Rectangular channels show superior performance
  - CRM surfaces perform comparatively better than CVM surfaces
- Bubble feeding mechanism at higher heat fluxes
- Rewetting phenomenon
  - Liquid filled corners in rectangular channels further enhances rewetting
  - Aids in extending the critical heat flux limits

Future Work

- Better manufactured sharper V-groove surfaces
- Porous surfaces over the open microchannels
  - Visualizations of bubble nucleation, growth and departure
- Experimentation under different:
  - Pressure conditions
  - Working fluids
- Testing of microchannel tube bundles, and study their effect on performance

Acknowledgement

Dr. Satish G. Kandlikar

Members of the Thermal Analysis, Microfluidics, and Fuel Cell Lab

Committee Members and Department Rep.

Dave Hathaway and William Finch

Robert Kraynik and Jan maneti

Dr. Edward Hensel and Mechanical Engineering Department Staff

Family and Friends

Thank you

Questions?

References

- [1] Incropera, F., Dewitt, D., Bergman, T., and Lavine, A., 2011, Fundamental of Heat and Mass Transfer, John Wiley & Sons, Inc.
- [2] Kreith, F., Manglik, R., and Bohn, M., 2011, Principles of Heat Transfer, Brooks/Cole.
- [3] Webb, R. L., and Pais, C., 1992, "Nucleate Pool Boiling Data for Five Refrigerants on Plain, Integral-Fin and Enhanced Tube Geometries," International Journal of Heat and Mass Transfer, 35(8), pp. 1893-1904.
- [4] Memory, S. B., Sugiyama, D. C., and Marto, P. J., 1995, "Nucleate Pool Boiling of R-114 and R-114-Oil Mixtures from Smooth and Enhanced Surfaces. I. Single Tubes," International Journal of Heat and Mass Transfer, 38(8), pp. 1347-61.
- [5] Huebner, P., and Kuenstler, W., 1997, "Pool Boiling Heat Transfer at Finned Tubes: Influence of Surface Roughness and Shape of the Fins," International Journal of Refrigeration, 20(8), pp. 575-582.
- [6] Tatara, R. A., and Payvar, P., 2000, "Pool Boiling of Pure R134a from a Single Turbo-Bii-Hp Tube," International Journal of Heat and Mass Transfer, 43(12), pp. 2233-6.
- [7] Rajulu, K. G., Kumar, R., Mohanty, B., and Varma, H. K., 2004, "Enhancement of Nucleate Pool Boiling Heat Transfer Coefficient by Reentrant Cavity Surfaces," Heat and Mass Transfer/Waerme- und Stoffuebertragung, 41(2), pp. 127-132.
- [8] Jung, D., Kwangyong, A., and Jinseok, P., 2004, "Nucleate Boiling Heat Transfer Coefficients of Hcfc22, Hfc134a, Hfc125, and Hfc32 on Various Enhanced Tubes," International Journal of Refrigeration, 27(2), pp. 202-6.
- [9] Jung, D., Lee, H., Bae, D., and Ha, J., 2005, "Nucleate Boiling Heat Transfer Coefficients of Flammable Refrigerants on Various Enhanced Tubes," International Journal of Refrigeration, 28(3), pp. 451-455.
- [10] Thome, J. R., and Ribatski, G., 2006, "Nucleate Boiling Heat Transfer of R134a on Enhanced Tubes," Applied Thermal Engineering, 26(10), pp. 1018-31.

References

- [11] Wen-Tao, J., Ding-Cai, Z., Nan, F., Jian-Fei, G., Numata, M., Guannan, X., and Wen-Quan, T., 2010, "Nucleate Pool Boiling Heat Transfer of R134a and R134a-Pve Lubricant Mixtures on Smooth and Five Enhanced Tubes," Journal of Heat Transfer, 132(11), pp. 111502 (8 pp.).
- [12] Chien, L.-H., and Webb, R. L., 1998, "Visualization of Pool Boiling on Enhanced Surfaces," Experimental Thermal and Fluid Science, 16(4), pp. 332-341.
- [13] Liang-Han, C., and Webb, R. L., 1998, "A Parametric Study of Nucleate Boiling on Structured Surfaces. I. Effect of Tunnel Dimensions," Transactions of the ASME. Journal of Heat Transfer, 120(4), pp. 1042-8.
- [14] Chien, L.-H., and Webb, R. L., 1998, "A Parametric Study of Nucleate Boiling on Structured Surfaces, Part II: Effect of Pore Diameter and Pore Pitch," Journal of Heat Transfer, 120(4), pp. 1049-1054.
- [15] Chien, L. H., and Webb, R. L., 2001, "Effect of Geometry and Fluid Property Parameters on Performance of Tunnel and Pore Enhanced Boiling Surfaces," Journal of Enhanced Heat Transfer, 8(5), pp. 329-339.
- [16] Nae-Hyun, K., and Kuk-Kwang, C., 2001, "Nucleate Pool Boiling on Structured Enhanced Tubes Having Pores with Connecting Gaps," International Journal of Heat and Mass Transfer, 44(1), pp. 17-28.
- [17] Kulenovic, R., Mertz, R., and Groll, M., 2002, "High Speed Flow Visualization of Pool Boiling from Structured Tubular Heat Transfer Surfaces," Experimental Thermal and Fluid Science, 25(7), pp. 547-555.
- [18] Chen, Y., Groll, M., Mertz, R., and Kulenovic, R., 2004, "Bubble Dynamics of Boiling of Propane and Iso-Butane on Smooth and Enhanced Tubes," Experimental Thermal and Fluid Science, 28(2-3), pp. 171-178.
- [19] Chien, L.-H., and Huang, H. L., 2009, "An Experimental Study of Boiling Heat Transfer on Mesh-Covered Fins," Proc. 2009 ASME Summer Heat Transfer Conference, HT2009, July 19, 2009 - July 23, 2009, San Francisco, CA, United states, 1, pp. 593-599.
- [20] Kotthoff, S., Gorenflo, D., Danger, E., and Luke, A., 2006, "Heat Transfer and Bubble Formation in Pool Boiling: Effect of Basic Surface Modifications for Heat Transfer Enhancement," International Journal of Thermal Sciences, 45(3), pp. 217-36.

References

- [21] Gorenflo, D., Baumhogger, E., Windmann, T., and Herres, G., 2010, "Nucleate Pool Boiling, Film Boiling and Single-Phase Free Convection at Pressures up to the Critical State. Part I: Integral Heat Transfer for Horizontal Copper Cylinders," International Journal of Refrigeration, 33(7), pp. 1229-1250.
- [22] Gorenflo, D., Baumhogger, E., Windmann, T., and Herres, G., 2010, "Nucleate Pool Boiling, Film Boiling and Single-Phase Free Convection at Pressures up to the Critical State. Part II: Circumferential Variation of the Wall Superheat for a Horizontal 25 Mm Copper Cylinder," International Journal of Refrigeration, 33(7), pp. 1251-1263.
- [23] Shou-Shing, H., and Tsung-Ying, Y., 2001, "Nucleate Pool Boiling from Coated and Spirally Wrapped Tubes in Saturated R-134a and R-600a at Low and Moderate Heat Flux," Transactions of the ASME. Journal of Heat Transfer, 123(2), pp. 257-70.
- [24] Cieilinski, J. T., 2002, "Nucleate Pool Boiling on Porous Metallic Coatings," Experimental Thermal and Fluid Science, 25(7), pp. 557-564.
- [25] Kim, J. H., Rainey, K. N., You, S. M., and Pak, J. Y., 2002, "Mechanism of Nucleate Boiling Heat Transfer Enhancement from Microporous Surfaces in Saturated Fc-72," Transactions of the ASME. Journal of Heat Transfer, 124(3), pp. 500-6.
- [26] Dominiczak, P. R., and Cieslinski, J. T., 2008, "Circumferential Temperature Distribution During Nucleate Pool Boiling Outside Smooth and Modified Horizontal Tubes," Experimental Thermal and Fluid Science, 33(1), pp. 173-177.
- [27] Mcneil, D. A., Burnside, B. M., Miller, K. M., and Tarrad, A. H., 2002, "A Comparison between Highflux and Plain Tubes, Boiling Pentane in a Horizontal Kettle Reboiler," 22, pp. 803-814.
- [28] Ribatski, G., and Saiz Jabardo, J. M., 2003, "Experimental Study of Nucleate Boiling of Halocarbon Refrigerants on Cylindrical Surfaces," International Journal of Heat and Mass Transfer, 46(23), pp. 4439-51.
- [29] Myeong-Gie, K., 2003, "Effects of Tube Inclination on Pool Boiling Heat Transfer," Nuclear Engineering and Design, 220(1), pp. 67-81.

References

- [30] Saidi, M. H., Ohadi, M., and Souhar, M., 1999, "Enhanced Pool Boiling of R-123 Refrigerant on Two Selected Tubes," Applied Thermal Engineering, 19(8), pp. 885-895.
- [31] Cooke, D., and Kandlikar, S. G., 2011, "Pool Boiling Heat Transfer and Bubble Dynamics over Plain and Enhanced Microchannels," Journal of Heat Transfer, 133(5).
- [32] Cooke, D., and Kandlikar, S. G., 2012, "Effect of Open Microchannel Geometry on Pool Boiling Enhancement," International Journal of Heat and Mass Transfer, 55(4), pp. 1004-1013.
- [33] Mehta, J. S., and Kandlikar, S. G., "Pool Boiling Heat Transfer Enhancement over Cylindrical Tubes, Part I: Experimental Results for Circumferential Rectangular Open Microchannels," International Journal of Heat and Mass Transfer.
- [34] Mehta, J. S., and Kandlikar, S. G., "Pool Boiling Heat Transfer Enhancement over Cylindrical Tubes, Part II: Experimental Results and Bubble Dynamics for Circumferential V-Groove and Axial Rectangular Open Microchannels," International Journal of Heat and Mass Transfer.